Atmospheric Electricity

https://www.iamas.org/icae/
NEWSLETTER
Vol.33 NO.2 Nov 2022

Positive cloud-to-ground lightning discharge that briefly coupled to a concurrent negative discharge 11 km away and whose recoil leaders caused luminosity dips instead of expected luminosity surges in the main channel to ground.

The image was obtained using a Phantom v310 high-speed camera running at 20,000 fps at the Lightning Observatory in Gainesville (LOG), Florida.

More details can be found in the paper by Ding, Z., Rakov, V.A., Zhu, Y. et al. Transient phenomena in positive cloud-to-ground lightning discharges. Commun Phys 5, 313 (2022). https://doi.org/10.1038/s42005-022-01087-8.

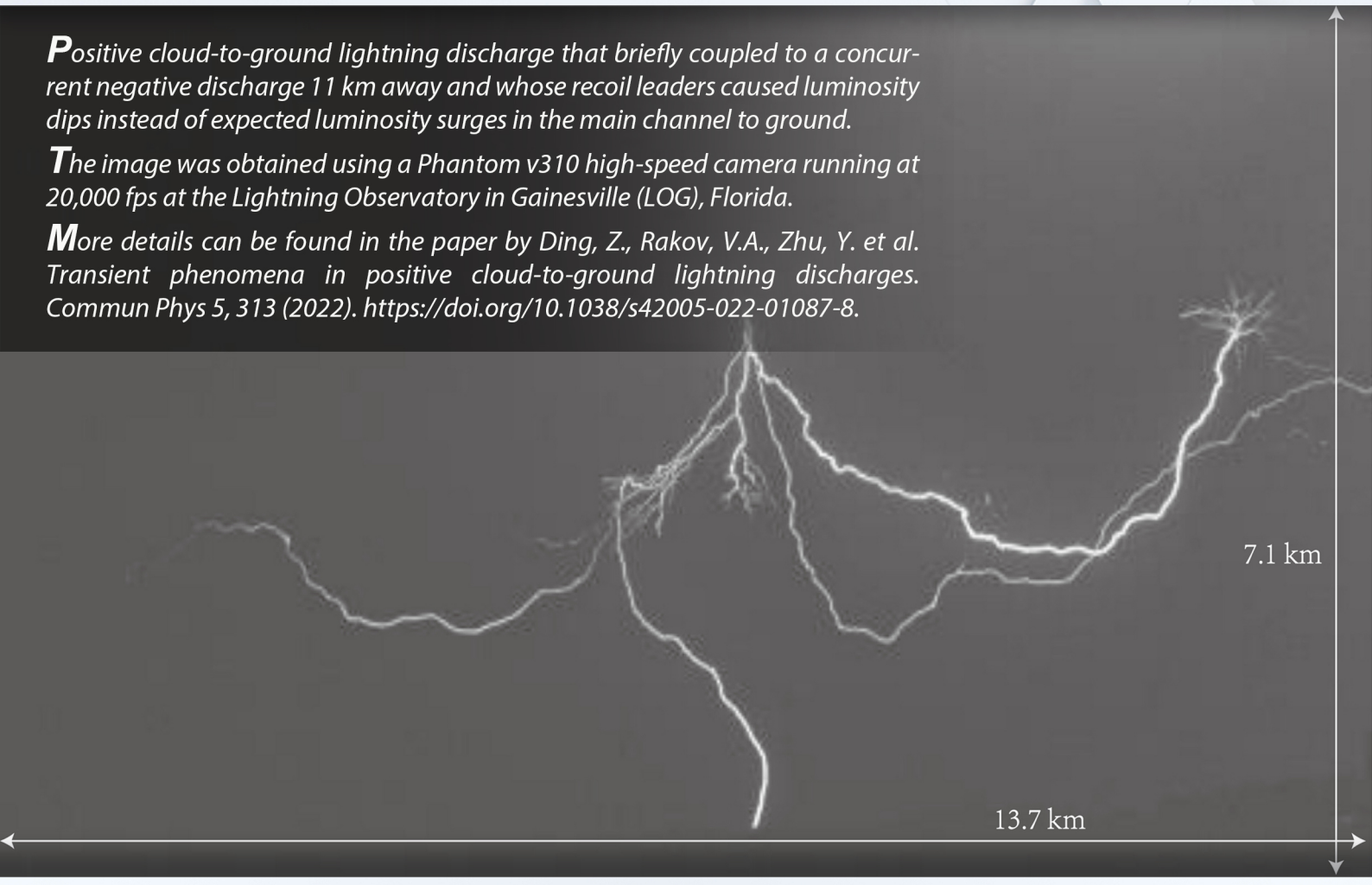

INTERNATIONAL COMMISSION ON ATMOSPHERIC ELECTRICITY
IAMAS IUGG
ICAE

Announcement of ICAE

During the 17th ICAE conference, the following three members have retired from their beloved commission (ICAE):
Vernon Cooray (Sweden)
Vladimir Rakov (USA)
David Smith (USA)

During the General Assemblies of ICAE Executive Committee, the ICAE Officers, three new members and two honorary members have been elected.
Xiushu Qie (President) and Weitao Lyu (Secretary) will continue to serve as ICAE officers for one additional period of 4 years.
Yoav Yair, Amitabh Nag, and Yasuhide Hobara have been elected as ICAE new members.
Vladimir Rakov and Clive Saunders have been elected as ICAE Honorary members.

Due to the above changes, the composition of new ICAE committee is as follows:
Officers:
President: Xiushu Qie (China)
Secretary: Weitao Lyu (China)

Committee Members (18):
Dr. E. Avila (Argentina), Dr. S. Cummer (USA), Dr. E. Defer (France)
Dr. U. Ebert (Netherland), Dr. G. Harrison (UK), Dr. Y. Hobara (Japan)
Dr. W. Lyu (China), Dr. D. MacGorman (USA), Dr. E. Mareev (Russia)
Dr. J. Montanya (Spain), Dr. A. Nag (USA), Dr. C. Price (Israel)
Dr. X. Qie (China), Dr. M. Saba (Brazil), Dr. M. Stolzenburg (USA)
Dr. T. Ushio (Japan), Dr. D. Wang (Japan), Dr. Y. Yair (Israel)

Honorary Members (12):
Dr. S. Anisimov (Russia), Dr. H. Christian (USA), Dr. J. Dye (USA)
Dr. Z-I. Kawasaki (Japan), Dr. P. Krehbiel (USA), Dr. E. Krider (USA)
Dr. P. Laroche (France), Dr. S. Michnowski (Poland), Dr. V. Rakov (USA),
Dr. C. Saunders (UK), Dr. S. Soula (France), Dr. E. Williams (USA)

The formal website of ICAE, **https://www.iamas.org/icae/**, has been updated.

After a series of procedures, **Barcelona, Spain** has been chosen as the venue of the next ICAE conference (18th conference), which will be held in **2026**.

Appointment of ICAE Representative on IAMAS ECS Committee:
Sonja Behnke, the first ICAE representative at IAMAS ECS (Early Career Scientist) committee, has been recently elected as president for ASE in AGU.
Rubin Jiang has been appointed by ICAE to succeed as the ICAE representative at the IAMAS ECS committee.

*I*CAE 2022 Summary

The 17th ICAE meeting was held successfully in Tel-Aviv, Israel, between 19-24 June, 2022. The venue at Tel-Aviv University's Porter School for Environmental Science hosted 120 participants from 30 countries. A total of 240 papers were initially submitted to the conference, and a 5-day scientific program of oral and poster sessions was created by the Local Organizing Committee after accepting reviews and recommendations made by the members of the ICAE Executive Committee. However, due to the evolving conditions of the Covid-19 pandemic and the difficulties it caused to international travel, as well as the restrictions caused by the Russia-Ukraine war, many papers and posters were withdrawn or cancelled. The final program contained 56 oral talks (some of which were pre-recorded) and 48 posters, arranged in 4 days. The social program included a half-day trip to the old city of Jerusalem and a Conference Dinner that included a dance competition between 4 teams of ICAE scientists and students in different music styles.

ICAE 2022 group photo

Awards

At the 36th International Conference on Lightning Protection (Oct. 2-7, 2022, Cape Town, South Africa), **Berger Award** was awarded to Daohong WANG and **Golde Award** was awarded to Ken CUMMINS.

The 28th IUGG General Assembly

The 28th General Assembly of the International Union of Geodesy and Geophysics will be held on 11-20 July 2023, at the CityCube Berlin, Berlin, Germany.

In IUGG2023, ICAE will organize three sessions:

M19: Lightning Observations for Research and Applications in Meteorology and Climate

Conveners: Eric Defer, Colin Price, Xiushu Qie

M20: Lightning Physics and Effects

Conveners: Maribeth Stolzenburg, Amitabh Nag, Weitao Lyu

M21: Thunderstorms and the Global Electrical Circuit

Conveners: Yoav Yair, Giles Harrison

A description of the sessions is given here https://www.iugg2023berlin.org/919-2/.

Some important dates:

10 October 2022	Online registration and abstract submission opens
	Online accommodation reservations open
	Travel grant applications open
14 February 2023	Closing of abstract submission
	Closing of grant application submission
17 March 2023	Abstract/grant acceptance sent to participants
28 April 2023	Early-bird registration closes
02 May 2023	Newsletter on field trips and accommodation reservations
12 May 2023	Complete scientific program and guidelines for presenters published

Looking forward seeing all in Berlin!

*E*GU2023 General Assembly

The EGU General Assembly will take place in Vienna on April 23-28th 2023 at the Vienna International Center (VIC).

On behalf of the co-conveners of session NH1.5: "Atmospheric Electricity, Thunderstorms, Lightning and their effect", I would like to extend a warm invitation to submit an abstract to this session. It is co-organized by AS1, co-sponsored by AGU and AGU-ASE.

The description and abstract submission are available at:

https://meetingorganizer.copernicus.org/EGU23/session/47019

Please choose NH1.5 and use your Copernicus ID to submit.

The deadline for submission is January 10th 2023 at 13:00 Central European Time.

We are looking forward to meeting you in person in Vienna next spring, for a great session.

Best regards,

Yoav Yair, Serge Soula, Karen Aplin, Sonja Behnke and David Sarraia

*T*he 12th Asia-Pacific International Conference on Lightning (APL 2023)

The 12th Asia-Pacific International Conference on Lightning (APL 2023) will be held in Langkawi, Kedah, MALAYSIA on 12-15 June 2023. The conference website is https://attend.ieee.org/apl-2023/.

*L*ightning and Climate

A recent publication by M. Fullekrug, E. Williams, C. Price, S. Goodman, R. Holzworth, K. Virts, and D. Buechler introduces lightning to the ‘State of the Climate in 2021’ (2.1 Lightning in Chapter 2 Global Climate, see link below).

https://www.ametsoc.org/index.cfm/ams/publications/bulletin-of-the-american-meteorological-society-bams/state-of-the-climate/

The World Meteorological Organization (WMO) recently declared lightning flashes to be an essential climate variable (ECV), based on a recommendation by the Task Team on Lightning Observation for Climate Applications (TT-LOCA) as part of the Atmospheric Observation Panel for Climate (AOPC) of the WMO and the Global Climate Observing System (GCOS). This endorsement reinforces the WMO Integrated Global Observing System (WIGOS) Vision 2040 toward the operational observation of lightning by space agencies during the coming decades.

The significance of this is that from now on, the Atmospheric Electricity community has the opportunity to contribute on an annual basis to the climate assessment by this scientifically oriented community. We think that this might be of interest to Atmospheric Electricians, given the ongoing deployment of lighting imaging sensors on geostationary satellites which are intended to serve this very purpose.

Sidebar 2.1: **Lightning**—M. FÜLLEKRUG, E. WILLIAMS, C. PRICE, S. GOODMAN, R. HOLZWORTH, K. VIRTS, AND D. BUECHLER

The World Meteorological Organization (WMO) recently declared lightning flashes to be an essential climate variable (ECV), based on a recommendation by the Task Team on Lightning Observation for Climate Applications (TT-LOCA) as part of the Atmospheric Observation Panel for Climate (AOPC) of the WMO and the Global Climate Observing System (GCOS; Aich et al. 2018; WMO 2019a). This endorsement reinforces the WMO Integrated Global Observing System (WIGOS) Vision 2040 (WMO 2019b) toward the operational observation of lightning by space agencies during the coming decades.

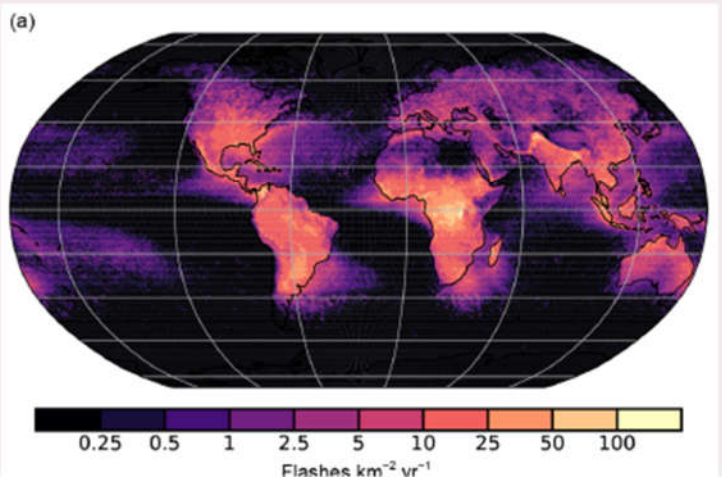

African Centres for Lightning and Electromagnetics Network (ACLENet)

ACLENet's mission is to decrease deaths, injuries and property damage from lightning across Africa. It was founded in Uganda in 2014 and incorporated as a nonprofit in both Uganda and the USA in 2016. We have been submitting updates to this newsletter since 2017 and are pleased to announce great strides since Covid has eased and travel is again possible for face-to-face meetings with government officials, schools, and other stakeholders. After two weeks of meetings, four staff members traveled with Dr Cooper, ACLENet's Director, to the International Conference on Lightning Protection (ICLP2022) in Cape Town, the first time ICLP has been held on the African continent. Pictorial reports on these activities can be seen at:

Strategic Partnership Meetings and A Life Changing Experience for ACLENet's Staff.

In order to transform the Memo of Understanding signed with the Ministry of Response, Disaster Preparedness (MoRDPR) in the Office of the Prime Minister of the Government of Uganda from a document and into a real partnership, Dr Mary Ann Cooper, president of ACLENet, traveled to Uganda in September to meet with government officials, visits schools, and work with staff. The MoRDPR and Prime Minister's office facilitated meetings with:

1. The Ministry of Energy, Uganda Institute of Professional Engineers, and other stakeholders to discuss the international Electrotechnical Commission standards, membership levels and adoption of IEC

standards for all new lightning and electrical work in Uganda.

2. The Ministry of Education and Sports to discuss design of lightning protection (LP) systems for new school construction, updating of older schools, lightning safety education working with teachers at the basic and secondary levels, and improvement and maintenance of lightning protection at existing schools.

3. Professor J.B. Kirabira, Director of the African Center of Excellence in Materials, Product Development and Nano-Technology, MAPRONANO, Uganda, at Makerere University, to discuss sourcing and qualifying of materials within Uganda to avoid the expensive importation of LP materials.

4. Brigadier General James Kinalwa, Head of the National Emergency Coordination and Operations Center, to discuss outreach to the communities most affected by lightning.

Other meetings included: 1. Rock View Primary School (LP system installed 2019-20, funded the Ludwig Family Foundation) to work with the science and math teachers for LP system maintenance. 2. Runyanya Primary School (LP system installed 2016-7) to commemorate International Lightning Safety Day, which had been delayed due to teacher strike and other problems.

*C*aribbean Meteorological Organization and Meteorological Service of Jamaica

In the Caribbean, the importance of lightning safety awareness has come to the forefront, particularly in Jamaica, where a number of lightning deaths occurred in 2020 and several casualties were reported since 2017. Motivated by those incidents, a peer-reviewed study of "Jamaica lightning occurrence, damage and casualties" was co-authored by Mr. Ron Holle (Holle Meteorology & Photography), Mr. John Cramer (Vaisala), Dr. Arlene Laing (Caribbean Meteorological Organization), and Mr. Evan Thompson (Meteorological Service, Jamaica), using Vaisala GLD360 lightning data.

The study found that during 2017-2021, lightning stroke densities were greater over the interior than along the coast of Jamaica. The seasonal activity is mostly from May through October, and, diurnal maximum is from 1200 to 1800 local time. The resulting impacts are considered by summarizing impact on infrastructure, sporting activity, and 18 human casualty reports resulting in 16 deaths and 39 injuries from 2005 through 2021. Most lightning casualties in Jamaica are males between 10 and 29 years old, occur between June and October, and in the afternoon. Common scenarios for

casualties are being close to trees, farming, playing soccer, and seeking safety inside small structures (Figure 1).

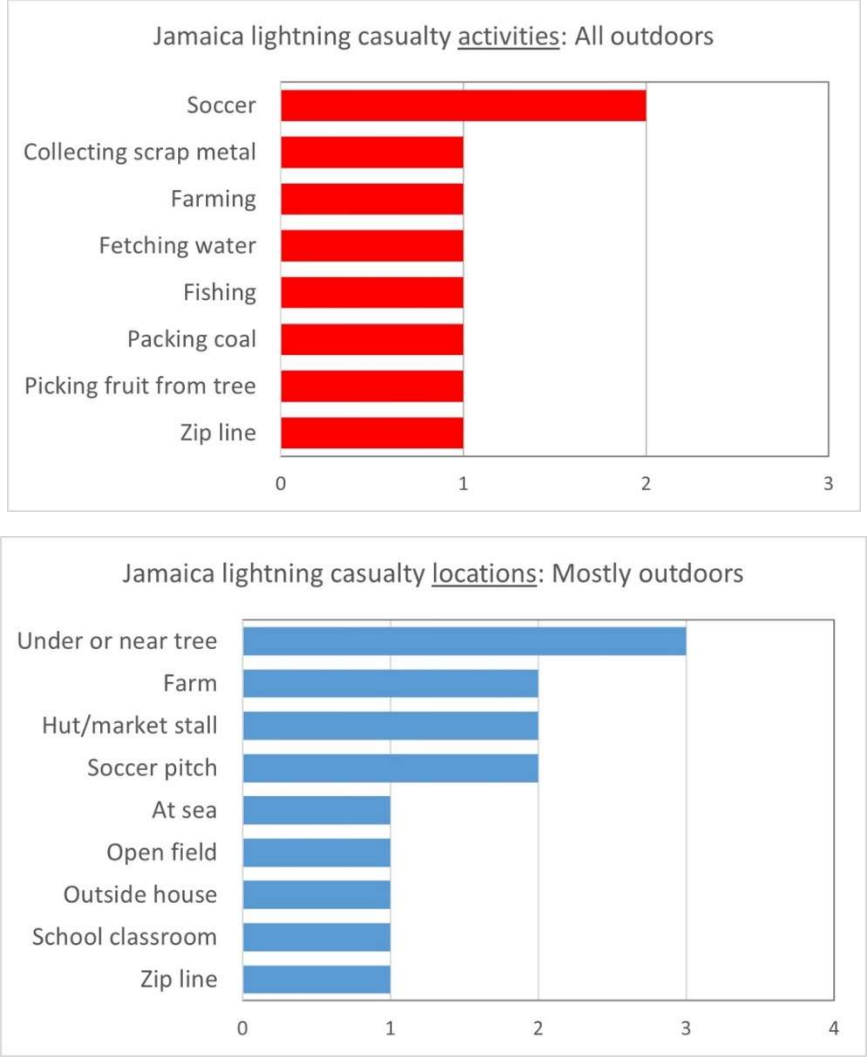

Figure 1. Activities and Locations of Lightning related casualties in Jamaica during 2005-2021.

The study was published by the IEEE and presented by the lead author at the 36th International Conference on Lightning Protection, 2-7 October 2022 in Cape Town, South Africa. The methods of this study could serve as a template for similar studies of other Caribbean countries and territories and motivate the establishment of a regional lightning detection network in the Caribbean. In addition, other Caribbean countries and territories are encouraged to collect comprehensive information on lightning-caused deaths, injuries, and property damage in order to more fully understand the nature of the threat in this region.

Department of Physics, Amrit Campus, Tribhuvan University, Kathmandu, Nepal and South Asian Lightning Network

Lightning threats in Nepal: occurrence and human impacts. Of all the natural disasters in Nepal, lightning has been recorded to be the second highest killer after earthquakes. Nepal's large topographical variation has a major influence on lightning occurrence and human casualties. Sharma et al. (2022) combined lightning detection by Vaisala's Global Lightning Dataset GLD360 network with lightning casualties from 2011 - 2020. Stroke density is least over high elevations to the north, moderate in hilly regions, and very frequent over the south. The Ministry of Home Affairs reports an average of 103 lightning deaths per year, and this fatality rate of 3.8 deaths per million per year is highest among South Asian countries. Fatalities over high mountains are rare, while most casualties are over central Nepal. (https://doi.org/10.1080/19475705.2021.2009922)

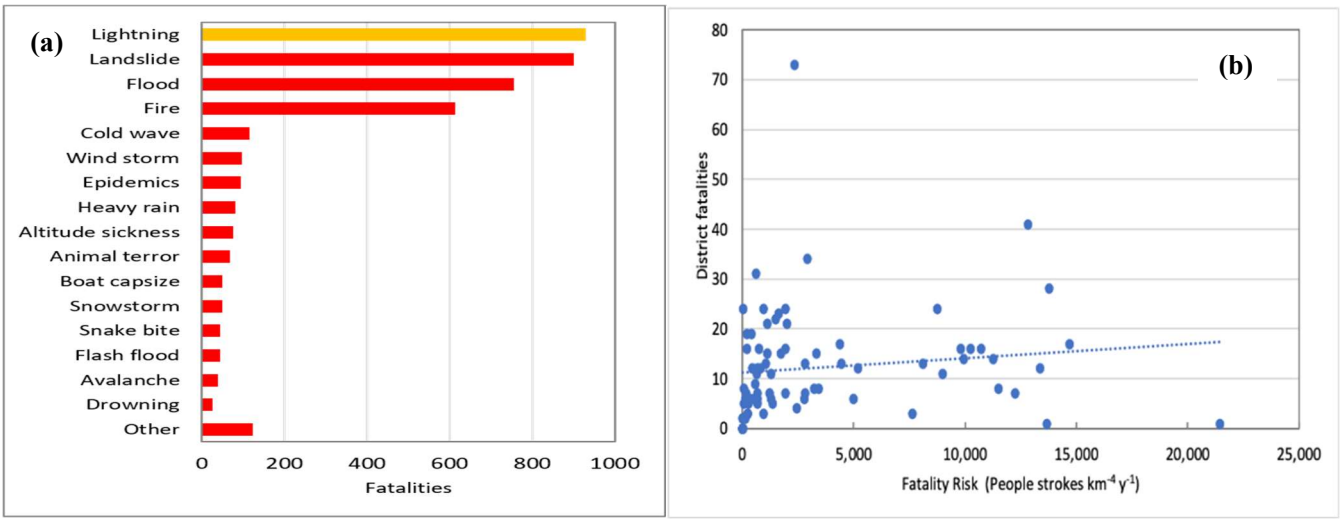

Figure 1. (a) Number of fatalities due to various natural disaster in Nepal, excluding earthquake (b) A plot of fatality risk due to lightning over the 77 districts of Nepal.

Archaeological sites in Nepal and India: concerns of lightning risks. At the October 2022 International Conference on Lightning Protection (ICLP) in Cape Town, South Africa, a review was made of lightning risks to a large number of archaeological sites in Asia. The study revealed that in most cases, no lightning protection measures have been adopted and, in several structures, protection was adopted without a risk assessment or standard system design under experts' advice.

Figure 2. Changunarayan temple located atop a small hill at Bhaktapur. The photograph depicts the down conductor dangling towards the bottom edge of the roof.

Lightning - a potential cause of house fires during the pre-monsoon season: a case study in Nepal. Another ICLP paper identified the locations and times of 13 house fires and matched them with lightning location data from Vaisala's Global Lightning Dataset GLD360 network. Lightning stroke density was greater closer to the fire locations than further away, which suggests that many fires attributed to electrical surges may have been initiated by lightning.

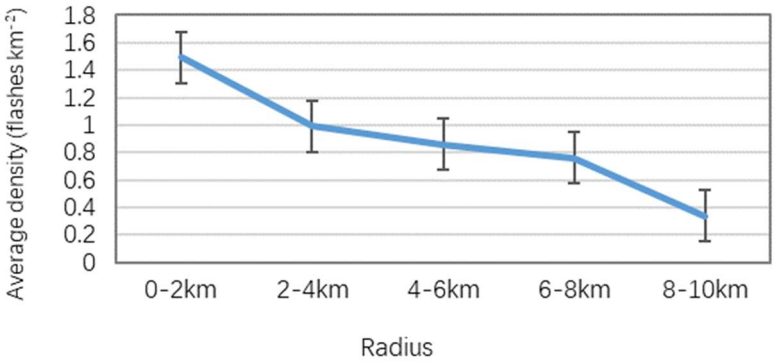

Figure 3. Average lightning stroke density versus radial distance of the lightning strokes from the reported house fire locations.

Distribution network impact assessment with geometrically identified strike points: an approach. A third ICLP study presented an algorithm to generate direct and indirect strike points for lightning impact assessments. The proposed method uses the Electrogeometric

Model to define the strike range limit, such that the generated events fall inside the range that would cause insulation failure. It is proposed that the commonly accepted fact that the impact level generally increases with the increasing arrester spacing, may not be always true.

The possible impact of atmospheric aerosol and other factors on lightning over the rugged terrain of Nepal. An additional paper at ICLP studied meteorological and atmospheric factors in generating thunderstorms over the mountains of Nepal. Atmospheric aerosol content and Convective Available Potential Energy (CAPE) were compared with stroke density from Vaisala' Global Lightning Dataset GLD360 network to measure thunderstorm activity. It was found that although CAPE and aerosols play significant roles in generating thunderstorms, they alone are not the determiner and that other climatic factors should also be considered.

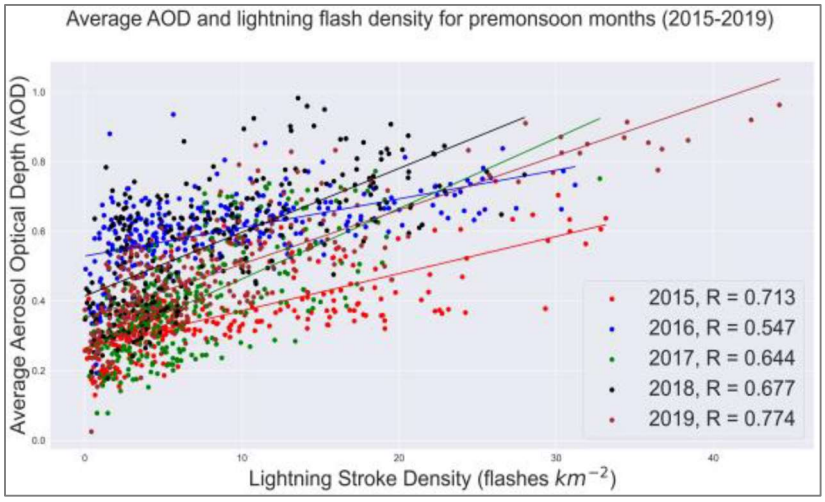

Figure 4. Example plots of correlation between the average value of Aerosol Optical Depth and lightning stroke density for the pre-monsoon periods 2015 - 2019. Highest correlation was for the 2019 pre-monsoon period and lowest for 2016.

*G*ifu University (Gifu, Japan)

A MF-HF 3D lightning mapping system for winter lightning observation. We have developed a 3D lightning mapping system with an array of Discone Antennas working in the medium frequency-high frequency (MF-HF) bands. This system is called discone antenna lightning mapping array (DALMA) and has been deployed in Hokuriku area of Japan for the

3D mapping of winter lightning. Radio waves in the MF-HF bands are rarely used for lightning 3D mapping due to large noises in these frequency bands. However, we have demonstrated that by using a wideband antenna, 3D mapping in the MF-HF bands can also produce satisfactory results. We have also discussed the advantages of DALMA compared with other 3D mapping systems in LF or very high frequency (VHF) bands. Figure 1 shows the 3D mapping result of a negative CG flash initiating a positive upward flash observed by the DALMA. This paper has been published in IEEJ Trans Elec Electron Eng. (https://onlinelibrary.wiley.com/doi/full/10.1002/tee.23667)

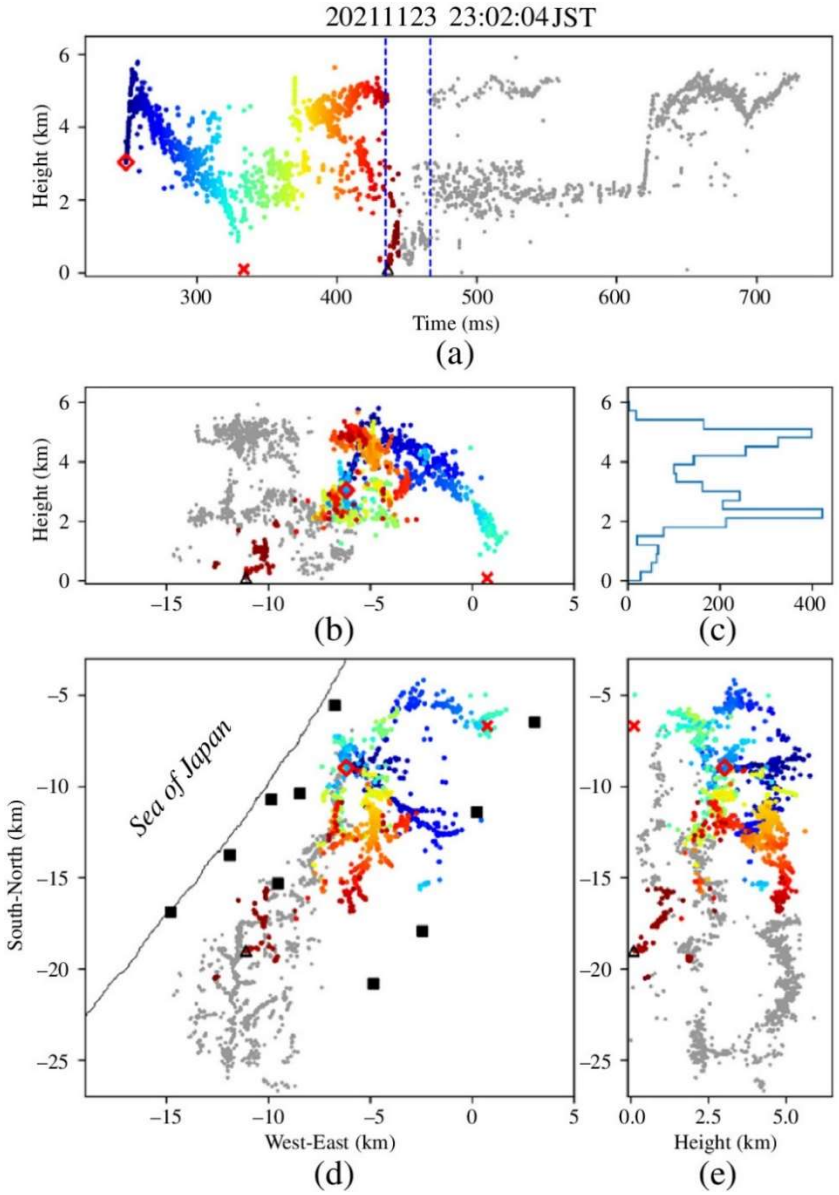

Figure 1. Three-dimensional mapping results of a negative CG flash initiating a positive upward flash. (a) Height-time view. (b) Height-distance (from west to east) view. (c) Distribution of located source

number at different heights. (d) Plan view. (e) Distance (from south to north)-height view. Sources up to the initiation of the upward negative leader from a tower are shown in color representing time, and sources after are shown in gray. The red diamond represents the first source of the CG flash. The red cross represents the negative return stroke. The black triangle represents the first source of the upward negative leader. Black squares represent observation sites of DALMA.

Intensity of first return strokes in positive cloud-to-ground lightning in winter. Intensities of about 700 first return strokes (RSs) in positive cloud-to-ground lightning flashes observed by a 14-site Fast Antenna Lightning Mapping Array in one winter season are analyzed. Peak currents estimated from range-normalized peak amplitudes of electric field change (E-change) waveforms of RSs are used to represent their intensities. It is found that peak currents of positive RSs are positively correlated with their waveform parameters including pulse width, rise time, fall time and half-peak width. Time differences between lightning initiation and first RSs are closely related with peak currents of positive RSs, with strong positive RSs usually associated with small time differences. Peak currents of positive RSs are also related with amplitudes of preceding leader pulses. Out of 674 positive RSs, 232 are preceded by positive leader pulses, and amplitudes of these pulses are positively correlated with peak currents of RSs. Strong positive RSs with peak currents larger than 150 kA are analyzed and compared with strong negative RSs. While strong negative RSs usually produce abnormal E-change waveforms that are generally different from typical RS waveforms, strong positive RSs do not have such special features. Strongest positive RSs usually occur within a very short time (usually smaller than 10 ms) after lightning initiation and are more likely to be associated with positive preliminary breakdown pulses. It is inferred that these strongest RSs are usually preceded by a fast downward positive leader with a speed on the order of 106 m/s. It is speculated that charge structures illustrated in Figure 2 are responsible for strong positive RSs. This study has been published in JGR Atmosphere.

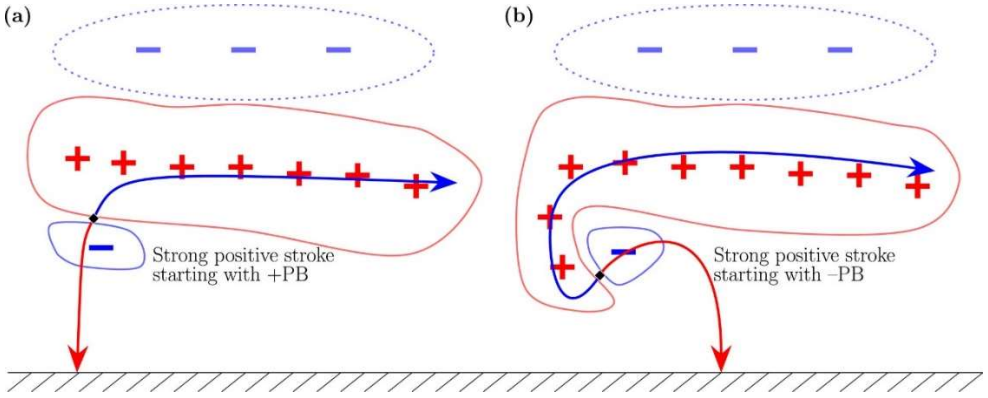

Figure 2. Illustrations of possible charge structures for strong positive strokes starting with (a) positive PB and (b) negative PB. Blue and red arrows represent negative and positive leaders, respectively.

Complicated aspects of a CG lightning flash observed in winter storm in Japan. Since the winter of 2018, we have conducted a new winter lightning observation campaign over the Hokuriku area in Japan with the simultaneous observation of multiple instruments, including high-speed video cameras, optical imaging systems LAPOS (Lightning Attachment Process Observation System), a lightning mapping system FALMA (Fast Antenna Lightning Mapping Array), etc. Recently, we have observed a CG lightning flash that exhibited several complicated aspects. The lightning flash lasted for about 0.34 seconds with a large horizontal extent of about 40 × 40 km. Based on the results of the FALMA and NAC, a sketch of the entire lightning flash observed is given in Figure 3. In the initial stage, two positive return strokes (RSs), labeled as +R1 and +R2, with remarkably different electric field change (E-change) waveforms were located with a horizontal distance of about 13.3 km. An upward positive leader (UPL) was triggered following the second positive RS from the tip of a tall tower. The UPL exhibited not only characteristic progression modes but also needle discharges. The results show a relation between the formation of needle discharges and the previous luminosity variation events (LVEs) of UPL. After the UPL entered the cloud, a negative leader connected with the UPL channel and resulted in a return stroke type of discharge that produced an E-change waveform similar to a large bipolar event (LBE) pulse. About 0.22 s after the UPL initiation, four negative RSs, labeled as -R1 to -R4, with two of them producing complicated E-change waveforms, were located at about 5.2 km from the tower. This study has been published in Journal of Atmospheric Electricity.

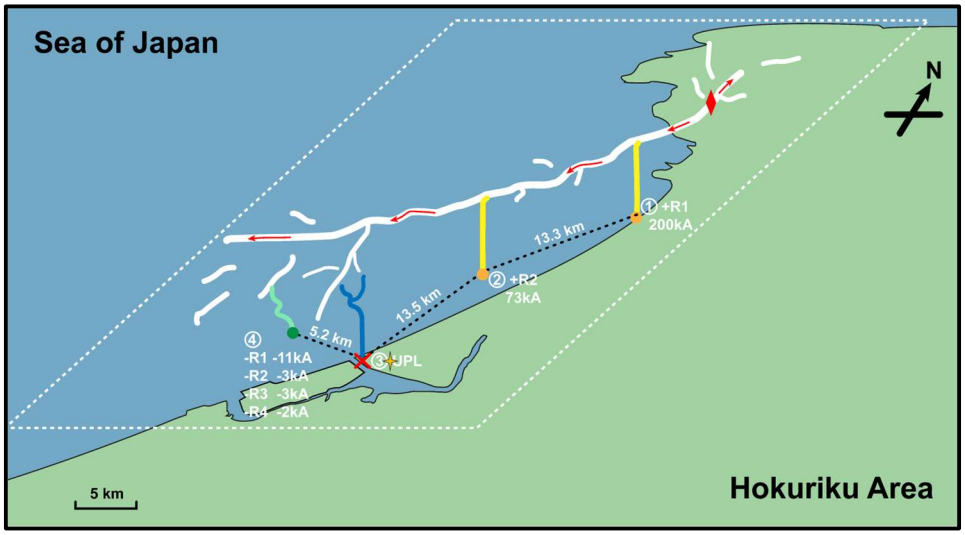

Figure 3. A sketch of the whole lightning flash. The locations of the tower and the optical observation site are shown with a red cross and a yellow quadrilateral, respectively. A white dotted parallelogram represents the layer of thundercloud. A red diamond and cross represent the lightning initiation location and the location of a lightning protection tower, respectively. White lines represent the leader inside thundercloud with red arrows representing the leader propagating directions. Other colored lines represent different discharge activities with the circled numbers referring to the corresponding sequence.

INPE, National Institute for Space Research, Brazil

In an effort to better understand the attachment process of cloud-to-ground flashes, the continuing currents in intracloud, downward and upward flashes and the high-energy radiation produced by lightning there are 3 international research collaboration projects in progress in USA, South Africa and Brazil:

High-speed video recordings of lightning associated with high-energy radiation. A research cooperation project between Dr. Rasha Abbasi from Loyola University in Chicago and Dr. John Belz from the University of Utah, USA and Dr. Marcelo Saba from INPE – National Institute for Space Research, Brazil. There we have high-speed video cameras in conjunction with the Telescope Array (TA) surface detector. Recently, we had the opportunity to capture a high-speed video of a lightning flash associated with a Terrestrial Gamma-ray Flash (TGF).

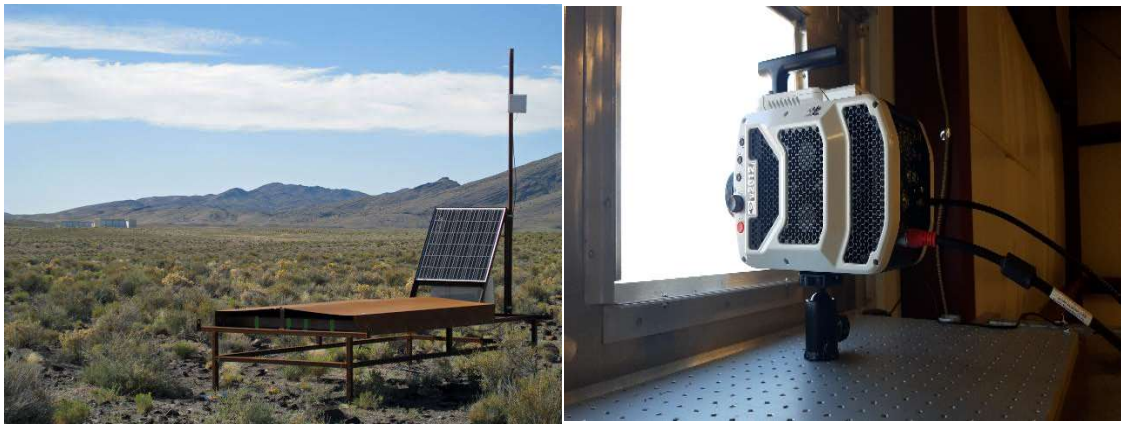

Figure 1. Gamma ray detector and high-speed camera installation in Utah.

High-speed images, electric-field, and current measurements of upward flashes from towers and attachment processes of downward flashes. A research cooperation project between Dr. Carina Schumann and Dr. Hugh Hunt from the University of Witwatersrand in Johannesburg, South Africa and Dr. Marcelo Saba Saba (INPE – National Institute for Space Research, Brazil).

Development of instrumentation to measure lightning (photometers, electric-field sensors, dataloggers). A research cooperation project between Dr. Miguel Guimarães, Dr. Listz Araújo and Dr. Rafael Alípio from CEFET – MG, Brazil with Dr. Marcelo Saba (INPE – National Institute for Space Research, Brazil) and Dr. Rasha Abbasi from Loyola University in Chicago.

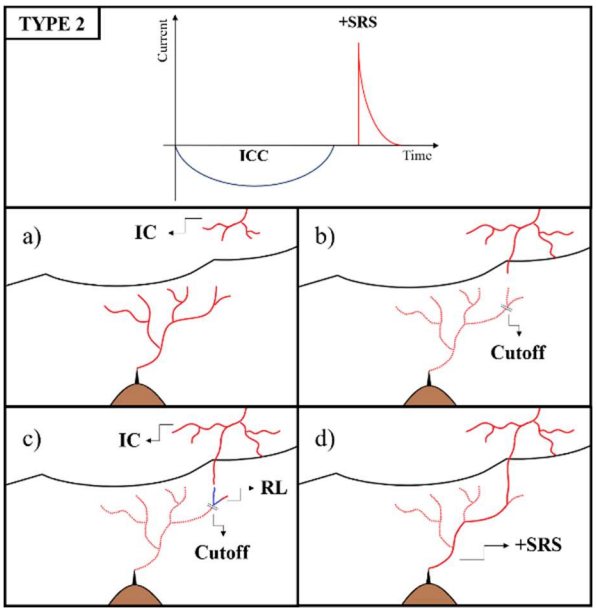

Figure 2. Schematic representation of the origin of the bipolar upward flash caused by the interaction of recoil leader (RL) with intracloud (IC) discharge (from Cruz et al., 2022).

*L*aboratory of Lightning Physics and Protection Engineering, State Key Laboratory of Severe Weather, Chinese Academy of Meteorological Sciences, Beijing, China

First measurements of low-medium frequency magnetic radiation for an altitude-triggered lightning flash. An altitude-triggered lightning flash was conducted on the Field Experiment Base on Lightning Sciences, China Meteorological Administration (CMA-FEBLS), in the summer of 2021. The low-medium frequency magnetic field (*B*-field) of altitude-triggered lightning was measured for the first time with a sensitive magnetic sensor. The *B*-field waveforms of precursors and sustained upward positive leader (UPL) show the obvious damped-oscillatory waveform, which is caused by propagation losses and reflections of lightning current at both extremities of steel wire. The propagation of UPL during the inception of attempted downward negative leader (DNL) is revealed by *B*-field signals with microsecond resolution, showing that the bidirectional leaders develop in an uncoordinated manner. The sustained DNL occurs about 5.5 ms after the inception of sustained UPL in our observations, and the measurements indicate that the stepping of DNL was much more frequent than that of UPL during the stage of sustained propagation.

Analysis of the configuration relationship between the morphological characteristics of lightning channels and the charge structure based on the localization of VHF radiation sources. The charge distribution within the horizontal charge region may have a more significant effect on the extension of the lightning channel. At present, it is still difficult to directly observe the charge structure of thunderstorm clouds, especially the horizontal charge structure. Also, the morphological study of the channel is not perfect due to the limitations of observation and data acquisition. Therefore, there is currently a lack of understanding of how lightning channel morphology reveals developmental characteristics and charge structure. In the paper, the relationship between the lightning channel morphology, developmental characteristics, and charge structure was investigated for the first time based on Lightning mapping array localization data, and the spatial distribution of the lightning fractal dimension (FD) was obtained. It is found that, compared to regions with unidirectional extended channels, regions with more channel branches or direction change of channel development have a larger FD and a higher power density, where horizontal channel development is accelerated. These correspondence features reflect the inhomogeneous presence of pocket charge, which provides a new method to use lightning morphology information to reveal the

characteristics of charge level distribution within thunderstorm clouds.

Spatiotemporal correlation between artificially triggered and adjacent natural lightning flashes. Triggered lightning flash (TLF) provides a unique perspective on the relationship between spatiotemporal proximity flashes, owing to its determined location and time, convenient direction measurement, and explicit association with the charge region. In this study, 3-D lightning location, current measurement, and atmospheric average electric field (AAEF) data were used to investigate the spatiotemporal relationship of TLFs (68 samples in South China) with adjacent natural lightning flashes (NLFs). The TLF-related negative charge regions had an average core height of 5.2 km and ambient temperature of approximately −1.7 °C. The effective negative charge region (the charge density that was high enough for the occurrence of lightning discharge) can be approximately equivalent to a circle with an average diameter of 10.3 km. For approximately 93% of (all) the TLFs, no NLF channel (initiation) was located within 5 km of the flash-triggered position, within 5 s before and after their occurrence. In situations where spatiotemporally adjacent NLFs and TLFs occurred, they were either associated with different charge layers, or the same charge layer but different charge positions. Most NLFs that caused significantly sharp AAEF changes just before or after the TLFs were not associated with the TLF-related negative charge. Therefore, the recovery of the AAEF, which has usually been referenced as the timing choice of the triggering operation, was not directly associated with the TLF-related charge region. The average interval between the TLFs and NLFs that occurred within 10 min before and after the TLFs and neutralized the TLF-related negative charge was approximately 145 s.

A 10-year thundersnow climatology over China. Thundersnow is a special kind of thunderstorm that combines snowfall and lightning. A 10-year thundersnow climatology over China was obtained based on observations during 2008–2017. Our results show that thundersnows are widely distributed in China, and most of the high-frequency areas are located in the Tibetan Plateau and northeastern China. The average frequency of thundersnow decreases with decreasing altitude, and thundersnow usually occurs at low-altitude stations once every 10 years. Thundersnow appears mostly in spring, autumn and late winter and can occur in high-altitude areas in summer. Thundersnow events increase the probability of blizzards, especially in the Shandong Peninsula in spring, North China and the Changbai Mountain in autumn, and the middle and lower reaches of the Yangtze River basin and Bohai Rim in winter. The percentage of positive cloud-to-ground lightning of winter thundersnow is approximately 20.7%, which is lower than those in other seasons. The negative phase of the

Arctic Oscillation and anomalous western North Pacific anticyclone are favorable background conditions for thundersnow events.

Lightning distribution in tropical cyclones making landfall in China. Lightning data from the World Wide Lightning Location Network (WWLLN) are used to document the lightning characteristics in tropical cyclones (TCs) making landfall in China. Data from a total of 74 TCs are collected from 2010 to 2020, providing 3293 individual time periods (1-h periods). WWLLN detected lightning activity in all TCs during the 48-h landfall, with lightning rates most frequently appearing between 250 and 600 str h^{-1}. Extreme hourly lightning rates of 3154 str h^{-1} and 4426 str h^{-1} are observed in the inner core and the outer rainbands respectively, comparable to lightning activity in mesoscale convection systems on land. TCs landing in Guangdong and Hainan have the largest peak lightning rates, while those landing in Zhejiang and Shanghai show the lowest lightning rates. The maximum lightning density is found in the inner core region of weak TCs (< 32.7 m s^{-1}) that are located approximately 100-200 km away from the coastline. The radial distribution of lightning density at landing stages is consistent with that at mature stages when TCs are over the ocean. However, there is a shift in the lightning maximum from the inner core prior to landfall (t_{-24}~t_0) to the outer rainbands after landfall (t_0~t_{+24}), indicating the effects of dry continental air intrusion and the enhanced surface frictional convergence. Vertical wind shear is the dominant factor in producing lightning and convective asymmetry for TCs landing in all locations. Lightning asymmetries are enhanced with the increase in shear magnitude from low (< 5 m s^{-1}) to moderate (5-10 m s^{-1}) and high (> 10 m s^{-1}) shear environments, both in weak and strong TCs (≥ 32.7 m s^{-1}).

Thunderstorm activity over the Qinghai–Tibet Plateau indicated by the combined data of the FY-2E geostationary satellite and WWLLN. Thunderstorm activity over the Qinghai–Tibet Plateau (QTP) has important climatic effects and disaster impacts. Using the thunderstorm feature dataset (TFD) established based on the black body temperature (TBB) and cloud classification (CLC) products of the Fengyun-2E (FY-2E) geostationary satellite, as well as the lightning data of the WWLLN, the temporal and spatial distributions and some cloud properties of the thunderstorms over the QTP were analyzed. Approximately 93.9% and 82.7% of thunderstorms over the QTP occur from May to September and from 12 to 21 o'clock local time, and the corresponding peaks are in August and at 14:00, respectively. There are three centers featuring frequent thunderstorms in the southeast, south-central, and southwest regions of the QTP. The average thunderstorm cloud area (the region with TBB ≤ −32℃) is 1.8 × 10^4 km^2. Approximately 32.9% of thunderstorms have strong convective cells (SCCs) composed of areas with TBB ≤

−52°C.The average number and area ratio of SCCs are 3.6 and 25.4%, respectively, and their spatial distribution is given. The average cloud area and the number and area ratio of SCCs of extreme thunderstorms (thunderstorms with the top 10% of lightning numbers) are approximately 30.0, 3.9, and 1.5 times those of normal thunderstorms. The spatial distribution of the thunderstorm activity is quite different from that of lightning activity given by the LIS and OTD over the northeastern and southwestern QTP, which may mean that the convection intensity, cloud structure, and charge structure of the thunderstorms over the QTP are different between different regions and seasons.

*L*ightning Research Group of Institute of Atmospheric Physics, Chinese Academy of Sciences (IAP, CAS), Beijing, China

Regional differences of convection structure of thunderclouds over the Tibetan Plateau. Tibetan Plateau (TP) is the highest plateau in the world, and also the source region of several major rivers and supports more than a billion people downstream. Thunderclouds are severe convective synoptic processes and significant contributors to the rainfall over the TP. To better estimate the impact of thunderclouds on the hydrological cycle and climatic system, it is necessary to understand the cloud structure and regional variation of thunderstorms over the TP. By using 17-year data of precipitation radar and lightning observations from TRMM satellite, the convective structures of thunderclouds over the TP are investigated in this paper. Significant differences of thunderclouds in terms of spatial distribution, seasonal variation, convective intensity and structure, are found in the eastern, central and western regions of the Plateau (namely ETP, CTP and WTP). From west to east, thundercloud increases in intensity and size. As indicators of thunderstorm intensity, flash rate, ice content, cloud top height and volume convective precipitation rate are all the largest in the ETP, while the average thundercloud frequency is the highest in the CTP. Thunderclouds in different seasons have different capacities of producing lightning with that in June over the ETP being the strongest. In terms of convective structure, the depth and horizontal areas of 20, 30 and 40 dBZ radar echo are the largest over the ETP, and the smallest over the WTP. The most remarkable difference among the three subregions is the horizontal area of 40 dBZ radar echo, the value of which over the ETP is about 2.6 times that over the CTP and 4.7 times that over the WTP, respectively.

Significantly increased lightning activity

over the Tibetan Plateau and its relation to thunderstorm genesis. Under the context of global warming, the frequency of lightning activity has changed a lot while space-based and ground-based lightning detection technology have provided unprecedented opportunities to understand the trends in lightning activity over the TP by their complementary and cross-validated advantages. This paper identified a significant increase in lightning activity in the last two decades over the TP, the highest plateau on earth, based on both OTD/LIS and WWLLN data. The largest rise of lightning activity was found over the region with high lightning density represented by the eastern TP at a rate of 0.072 ± 0.069 fl km $^{-2}$ yr $^{-1}$ during 1996–2013 from OTD/LIS. WWLLN data also showed a remarkable increase in lightning strokes during 2010–2019 in the maximum lightning density region, while the change was insignificant in the low lightning density region (Figure 1). Further investigations revealed an interesting result that most of the TP region experienced a significant increase in thunderstorm frequency, which was responsible for the increase in lightning activity, rather than an increase in thunderstorm intensity. Increased lightning activity implies a potential risk to human beings and the fragile ecosystem over the TP in a warmer climate.

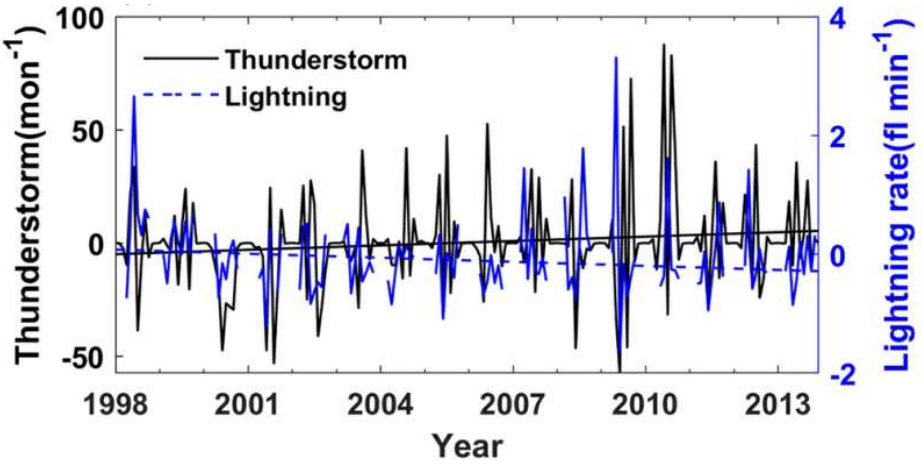

Figure 1. Trends of thunderstorm frequency and lightning rate in a thunderstorm during 1998–2013 over the eastern Tibetan Plateau. The time series of thunderstorm anomaly (black lines; units: mon $^{-1}$) and anomalous lightning rate in a thunderstorm (blue lines; units: fl min $^{-1}$).

Combined assimilation of radar and lightning data for the short-term forecast of severe convection system. A lightning data assimilation (LDA) method adjusting dynamical fields was examined in the rapid cycle with Weather Research and Forecasting (WRF) model and WRF Data Assimilation (WRFDA). This method retrieves pseudo vertical velocity profiles from total lightning observations and promotes wind convergence over lightning

regions. This newly developed LDA scheme is compared with radar data assimilation (RDA) that has been routinely applied in severe storm nowcasting models. Depending on whether the radar or lightning data is assimilated, four experiments were designed to evaluate the positive impacts of dynamical adjustment from LDA. The effects of RDA and LDA are different by using a typical severe mesoscale convection system occurred in Beijing. The assimilation of radar radial velocity mainly improves the forecast in a longer time, while assimilation of pseudo-vertical-velocity from lightning data mainly corrects intensity and location of the forecasted precipitation. When both radar and lightning data are assimilated, the small-scale wind convergence are promoted and contributes to the intensified updrafts. Thermal and water vapor fields are also adjusted indirectly. Consequently, the convective precipitation is significantly improved and the positive impacts from the combined assimilation scheme persisted over a longer period (at least 3 hours). It can be concluded that a combined assimilation of convective data from multiple sources such as radar and lightning data enhance prominently the accuracy of short-term convection forecasts.

Lightning VHF radiation mapping method for an irregular short-baseline array. Lightning VHF interferometry is a crucial tool for studying the development of lightning leaders within thunderclouds, and the conventional antenna array is composed of two coplanar orthogonal baselines. In this study, we developed two new location methods for an irregular array based on the optimization algorithm, using all baselines in the calculation. We analyzed the effects of two kinds of time uncertainty on the location result and provided a calibration method. The first type – the systematic time drift of antennas – can induce an offset on the location result, leading to a worse accuracy. We can calibrate the time drift of each antenna efficiently during the experiment. The second type – the waveform distortion between different antennas – can introduce the noise on time, leading to worse precision. The location precision improves when more baselines are used, whether they are independent or redundant. Our result shows that the non-coplanar configuration can significantly improve the elevation uncertainty near the horizon and the azimuth uncertainty near the zenith after considering the angular uncertainty's theoretical distribution. Therefore, a non-coplanar short-baseline array could be a new and promising approach and research field, in particular, for studying the attachment process and CG strikes at low elevation or IC lightning process at the zenith (Figure 2).

Aerosol impacts on storm electrification and lightning discharges under different thermodynamic environments. The impacts of aerosol and thermodynamics on electrification and lightning activities have been investigated in detail using the WRF model coupled with a

double-moment microphysics parameterization and an explicit electrification lightning scheme. Varied combinations of CAPE values and aerosol concentration were considered in the simulations. The results showed that the electrification and lightning activities vary under different thermodynamic and aerosol conditions. Under high CAPE circumstances, the augmentation of ice-phase particle leads to the enhancement of non-inductive charging primarily through the dynamic processes. Elevated aerosol loading under lower CAPE conditions invigorates lightning activities due to larger graupel particles produced by increased cloud droplet and ice crystals, which participated in the thunderstorm electrification.

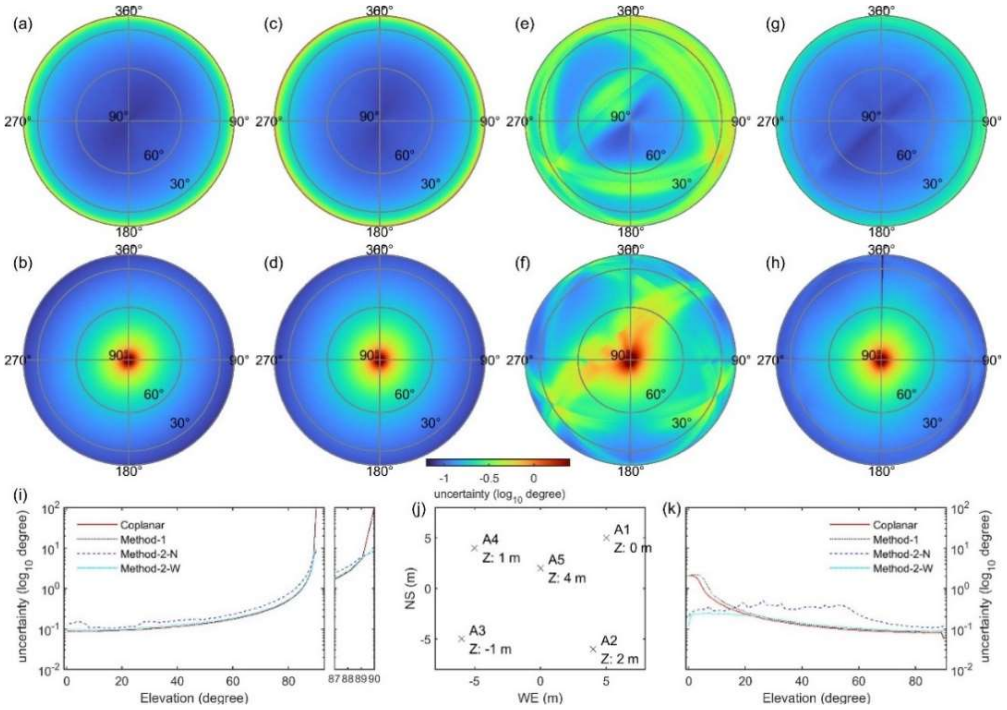

Figure 2. Comparison of uncertainty distribution of a five-antenna non-coplanar array using different methods. Elevation uncertainty (a) and azimuth uncertainty (b) for the coplanar array by setting the altitude of all five antennas as zero. Elevation uncertainty (c) and azimuth uncertainty (d) by Method 1 of constraint optimization. Elevation uncertainty (e) and azimuth uncertainty (f) by Method 2 of coordinate rotation using the arithmetic average. Elevation uncertainty (g) and azimuth uncertainty (h) by Method 2 of coordinate rotation using weight average. Azimuth uncertainty (i) and elevation uncertainty (k) of different methods along the azimuth of 60°. (j) Configuration of the five-antenna non-coplanar array.

Transient luminous events and lightning strokes over the Tibetan Plateau and its comparison regions. The relationship between transient luminous events (TLEs) and lightning strokes over the TP, and its comparison regions as Yangtze-River Delta (YRD) and East China Sea (ECS) at the same latitude belt are investigated by using the observations from the Imager of Sprites and Upper Atmospheric Lightning (ISUAL) and WWLLN. Although the relative weak convective system and less intense lightning over the TP are well known, elves, sprites and halo, mostly occurred in August and September, were detected over its southeast area. Different from the TP, the detected number of sprite and sprite-to-stroke ratios over the YRD are larger in spring than in summer and autumn. The monthly halo distributions display their frequent occurrences in August over all the study regions. Blue jets only detected over the YRD with the frequent events in August and September, with the jet-to-stroke ratios being larger than the ratios of sprite-to-stroke and halo-to-stroke. The average peak current of TLEs-related lightning strokes over the TP is larger than those over the YRD and ECS. The TLEs-producing thunderstorms are high clouds (at the altitudes of 12-14 km) over all study regions, those of which over the TP are around 1 km higher with less cloud ice water content than those over the YRD and ECS. The feature of air dynamics displays the convective of TLEs-producing thunderstorms over the TP is weaker than those over the YRD and ECS.

*M*assachusetts Institute of Technology

The study led by Hungarian collaborators Jozsef Bor, Tamas Bozoki and Gabriella Satori on the comparative global circuit response of the superlative Tonga eruption of January 15 2022 has been submitted to the Journal of Geophysical Research. As a follow-up to that work, tephigram analysis of the record-breaking overshooting of the stratosphere (to a maximum height of 58 km) by this eruption in the interval 0400-0430 UT allows for the possibility of supersonic ascent. Video clips taken by Mary Lyn Fonua (Matangi Newspaper, Tonga) with sounds resembling gunshots and cannon fire may be sonic booms emanating from the inferred rapid ascent. Similar sounds were documented in conjunction with another superlative eruption at Krakatoa in 1883 (Symons, 1888).

The availability of a global land surface temperature dataset (berkeleyearth.com) has enabled new investigations of the AC global circuit response to global temperature. Preliminary results were presented at the GLM Science Meeting at NASA in September for 19

consecutive days in 2019. A drop in global lightning activity by more than a factor-of-two is now attributed to a cold air outbreak from the Arctic that impacts both the American and the African chimneys. GLM-based flash totals in the Amazon basin were reduced by a factor-of-two. These results will also be shown in a poster led by Yakun Liu at the upcoming AGU meeting.

Anirban Guha visited MIT for one month earlier this fall and completed a project long in the planning stage: the automated geolocation of Schumann resonance "bell-ringers", transient excitations of the Earth-ionospheric cavity that send energy around the Earth multiple times. Special use is made of the six-station HeartMath ELF network, with identical magnetic sensor pairs in California, Canada, Lithuania, Saudi Arabia, South Africa and New Zealand. Hyperbolic ranging on a sphere has been implemented for this purpose based on GPS time stamping of every data sample. It is anticipated that this new capability will be useful for testing the so-called symbolic equations involving different ionospheric heights in daytime and in nighttime conditions.

During the same visit noted above, further consideration has been given to the value of a pair of magnetic coils at the South Pole for a single-station monitoring of the Earth's Schumann resonances and global lightning activity. Given the fortuitous separation of the three continental lightning "chimneys" by 90°, 90° and 180°, one coil can be favorably oriented for Africa reception, and the other perpendicular coil oriented for Asia/Maritime Continent and South America, but with peak reception separated in time by 12 hours. Two key virtues of this unique site is that all chimney sources are roughly equidistant from the receiving coils, and the condition of the local ionospheric height (day vs night) is the same for all three chimneys.

Northwest Normal University, China

The initial radius of lightning return stroke channel and its relation with discharge intensity. The radius of the lightning channel is one of the major parameters that closely related to lightning discharge characteristics. The initial radius of the return stroke is an important parameter reflecting lightning discharge intensity. Based on spectral diagnosis and electrostatic approximation of the vertically descending leader model, the lightning channel temperature, line charge density, and electrostatic energy of seven dart leader-return stroke sequences were estimated. Finally, the initial radii of the return strokes were obtained. We analyzed the relationship between the initial radii and the corresponding discharge

parameters. The initial radius is found to have a good linear correlation with each of the following quantities: the line charge density of the dart leader, the total intensity of ionic lines in the spectra, and the optical radius, as shown in Figure 1. It is also inversely proportional to the leader duration. These correlations confirm that the initial radius is closely related to discharge intensity, and that the charge stored in the leader channel directly determines the initial radius and discharge intensity of the return stroke.

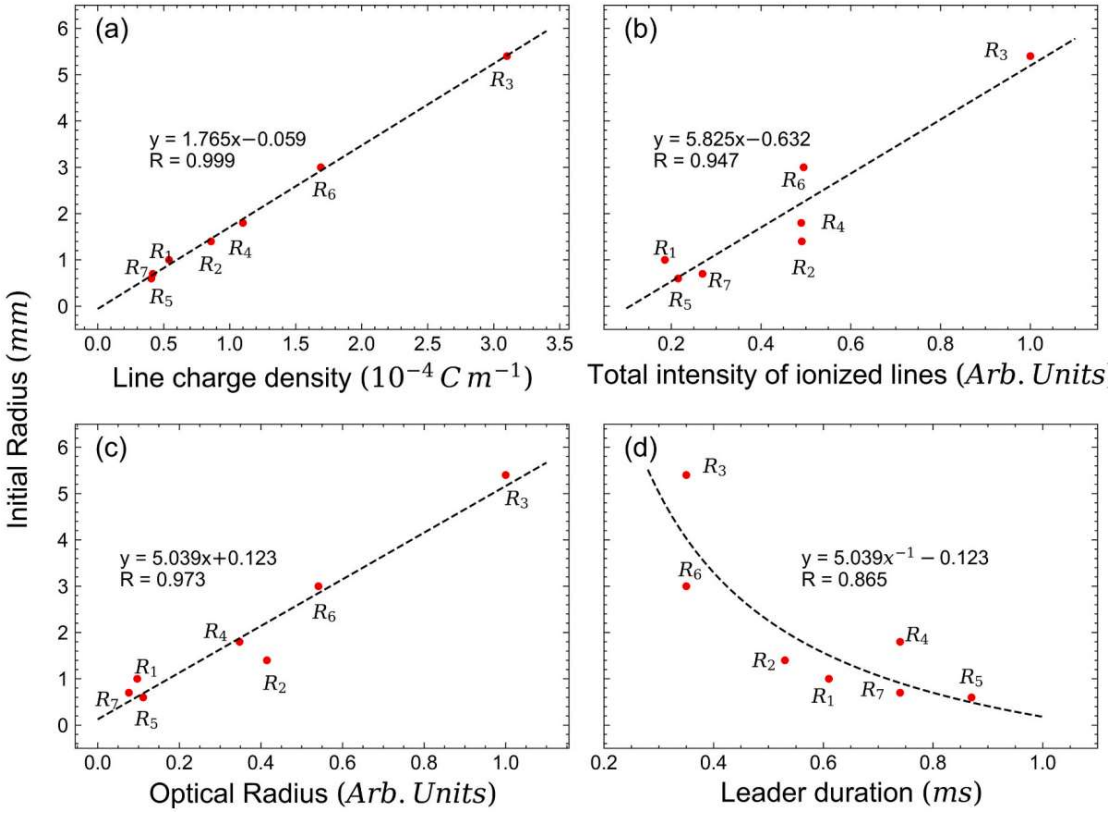

Figure 1. The relationship between the initial radius and each of the following parameters: the line charge density, total intensity of ionic lines in the spectra, optical radius, and leader duration.

The influence of leader charge on current intensity and spectral characteristics of return strokes. The characteristic parameters reflecting the current intensity in lightning return stroke discharge channel are the primary concern in the field of lightning physics research and protection. The leader charge quantity is one of the key factors affecting the peak current of the return strokes. Based on the spectrum and the corresponding fast electric field change waveforms for 9 natural cloud-to-ground lightnings including multiple return strokes, part of the total charge quantity in the corresponding leader channel was estimated by different methods, and its influence on current intensity and spectral characteristics of return strokes

were further investigated in this work. The results show, that for the same lightning, part of the leader charge quantity estimated by using the two methods according to the electric field change waveforms is in good agreement with the electron number per channel length calculated by basing on leader spectrum, it is also found that part of the neutralized leader charges is positively correlated with the peak current, the radius of the core current-carrying channel and the total intensity of ionic lines in the spectrum. These results verified that the current intensity of the lightning return stroke discharge mainly depends on the charge quantity being stored in the previous leader process. The radius of the core current-carrying channel is closely related to the current intensity. Moreover, the intensity of the ionic line in the spectrum can directly reflect the current intensity.

*R*eichman University

The analysis of the data received from the successful ILAN-ES experiment conducted in April 2022 during the Rakia mission on the International Space Station is led by Yoav Yair and students from Reichman University. The operational procedure for lightning target forecasts practiced during the mission showed > 90% accuracy in predicting thunderstorm locations relative to the ISS track. Out of 84 targets requested for astronaut directed observations, 22 were granted by NASA and imaged with a Nikon D6 camera, yielding a total downloaded (usable) video of ~ 155 minutes. The total number of detected TLEs (unambiguously identifiable) was 46 events: 10 Sprites, 1 Sprite Halo, 10 Elves and 25 BLUEs. Matching the events with ENTLN and WWLLN lightning locations and meteorological data is on-going and submitted for publication in due time.

*U*niversity of Florida

Z. Ding, S. Chen, V.A. Rakov, Y. Zhu, I. Kereszy, and M.A. Uman authored a paper titled “Comparison of far electric field waveforms produced by rocket-triggered lightning strokes and subsequent strokes in natural lightning”. Using wideband electric field records obtained at the Lightning Observatory in Gainesville (LOG), Florida, they examined in detail the

characteristics of far electric field waveforms produced by two categories of lightning return strokes. The first category includes return strokes of any order in lightning flashes triggered by a rocket extending a grounded wire toward the overhead thundercloud, which they label RTL (rocket-triggered lightning) strokes. The second category includes return strokes of order 2 and higher (that is, only subsequent strokes) in natural cloud-to-ground lightning flashes, which they label NL (natural lightning) strokes. Properties of RTL and NL strokes are expected to be similar, and RTL strokes are often assumed to be representative of NL strokes. A total of 139 RTL strokes from years 2013 to 2016 and 184 NL strokes from years 2013 to 2015 were examined in this study. All strokes transported negative charge to ground and occurred at similar distances from LOG. Similarities and dissimilarities of waveform parameters for the two categories of strokes and their possible explanations are discussed in this paper. Far electric field waveforms for RTL strokes tend to be narrower and rise to peak faster than those for NL strokes. The corresponding statistical distributions for RTL strokes are less dispersed than for NL strokes. The differences in AM values are statistically significant and their explanations are offered in the paper. This is the first detailed comparison of electric field waveforms of RTL and NL strokes recorded at approximately the same distance (some tens of kilometers) and with the same instrumentation. The paper is published in the Special Issue of Electric Power Systems Research (EPSR) devoted to ICLP-SIPDA 2021.

V.A. Rakov and I. Kereszy authored a paper titled “Ground-based observations of lightning-related X-ray/gamma-ray emissions in Florida: Occurrence context and new insights”, which is based on (is an extended version of) the Invited Lecture given by the authors at the ICLP-SIPDA 2021 in Colombo, Sri Lanka. The authors presented and discussed ground-based observations of energetic radiation (X-rays/gamma-rays) associated with natural lightning discharges. The emphasis is placed on relating X-ray/gamma-ray emissions to specific lightning processes. X-rays/gamma-rays have been observed in the following three contexts: (1) final stages of the descending leader, (2) collision of opposite-polarity streamers at the onset of lightning attachments process, and (3) in-cloud processes giving rise to energetic radiation bursts characteristic of Terrestrial Gamma-ray Flashes (TGFs). It appears that the X-ray/gamma-ray production can be materially influenced (enhanced) by the presence of previously created but decayed lightning channels. Such channels are characterized by elevated temperature (about 3,000 K vs. 300 K for ambient air), which significantly lowers channel air density and modifies the friction curve (representing the spatial rate of electron energy loss), so that its peak is an order of magnitude lower than that for cold air. As a

result, in the electric field of about 4 MV/m (such and even higher fields are briefly produced near the tips of lightning leaders; e.g., Kereszy et al., Appl. Sci., 2022), ambient electrons can be accelerated over the friction-curve peak to the keV range and further to relativistic energies needed for production of X-ray/gamma-ray emissions. Significant avalanching of runaway electrons seems to be possible. For one very intense (55 kA) subsequent stroke, which was a prolific X-ray/gamma-ray producer, the spatial extent of strong (>4 MV/m) electric field region associated with the descending leader tip was estimated to be about 1.5 m, which is sufficient for multiplication of runaway electrons by a factor of 2×10^4 or so. All downward TGFs observed in Florida (a total of five to date) occurred well after the flash-initiation process, in contrast with the observations of downward TGFs in Utah and Japan. The paper is published in the Special Issue of Electric Power Systems Research (EPSR) devoted to ICLP-SIPDA 2021.

*U*niversity of Texas

At the University of Texas at Dallas, Prof. Brian Tinsley, who retired in 2011, continues to dabble in research on the connection between small changes in the global electric circuit downward current density, J_Z, and small changes in weather. These suggest overall larger unappreciated effects on cloud microphysics and climate. The effects are interpreted as being due to electrostatic charge accumulation on aerosol particles and droplets in clouds, due to cosmic ray ion production generating charge pairs, and J_Z generating space charge by concentrating positive charge at cloud tops and negative charge at cloud bases. The charges result in electro-antiscavenging of small aerosol particles in the space charge regions which mixing redistributes into the clouds, and electo-scavenging of larger aerosol particles (condensation and ice-forming nuclei), independent of space charge.

A paper reviewing and updating observational results on clouds, and the atmospheric dynamical changes due to cloud radiative forcing, was published recently in JGR-Atmospheres. Prof. Tinsley is currently analyzing cloud and atmospheric dynamical responses to Forbush decreases of the cosmic ray flux, which also appear capable of being understood in terms of J_Z changes (doi:10.1029/2021JD035954).

*U*niversity of Zambia

Contributors: Shadreck Mpanga, Ackim Zulu, Mabvuto Mwanza, Ronald L. Holle, Mary Ann Cooper

Understanding the Lightning Phenomenon in Zambia. There is an improved understanding of the lightning phenomenon in this part of central southern Africa. The meeting of lightning safety advocates in Lusaka, the capital city of Zambia, in September 2015 added impetus to the need to pay more attention to the effects that lightning causes on the infrastructure around the country. In 2016 Zambia adopted the standard series, IEC 62305-3 and IEC 62305-4, as the apex documents for the implementation of lightning protection system (LPS) designs for various buildings around the country. In 2018, the African Centres for Lightning and Electromagnetics Network (ACLENet) started publishing monthly articles on the lightning phenomenon and some practical works being done to protect communities against the effects of lightning strikes especially in countries like Uganda. The works being done in this country are being seen by other African countries and they are likely to learn from them. ACLENet exchanges notes on best practices with its sister network in Asia called South Asian Lightning Network (SALNet). They do this through online meetings where experts in the field present on case studies and latest developments on LPS installations. Zambia learns from all these undertakings. ACLENet is headed by Professor Mary Ann Cooper, formerly of the University of Illinois at Chicago whereas SALNet is headed by Professor ShriRam Sharma from Tribhuvan University in Kathmandu, Nepal. The two friends, seen on the right in the photo below, recently met at the ICLP held in South Africa from 2-7 October 2022.

Figure 1. Lightning advocates from around the world at the ICLP conference in South Africa (Source:

ACLENet website) From the left: Gopa Kumar (India), Ron Holle (USA-ACLENet), Chandima Gomes (Sri Lanka-Malaysia-South Africa), Mitchel Guthrie (USA, ACLENet), Cooper (USA-ACLENet), and Sharma (Nepal, SALNet)

The other four members in Figure 1 are the pioneers of LPS and lightning science that help the leaders of ACLENet and SALNet with spreading lightning awareness around the continent of Africa, Zambia included. Due to the efforts of these pioneers and the no-cost policy for the lightning data when a university researcher applies to Vaisala Inc. for lightning information, it was possible for a researcher from the University of Zambia (UNZA) to give an online presentation on the 'Improvement of LPS design parameters for buildings in Zambia' during the ICLP on 6th October 2022. The improved parameters per province are as shown in Figure 2. The importance of these parameters is explained by an algorithm that contains equations 1 to 3 where A_e is the area of an installation, a building in this case, to be assessed for the possibility of installing an LPS, L is the length of the building, W the width and H the height. Furthermore, N_d is the expected yearly lightning strike frequency to the building with area A_e, N_g is the lightning flash density and is the parameter determined in Figure 2 for each province in the country, C_1 is the environmental coefficient, C_2 the structure coefficient, C_3 the structure contents coefficient, C_4 the structure occupancy coefficient and C_5 the lightning strike consequence coefficient. These five coefficients can be found in tables provided by standards on lightning protection of infrastructure such as NFPA 780 and IEC 62305-3. C_2, C_3, C_4 and C_5 are used to determine the tolerable lightning strike frequency N_c to a building as shown in equation 3.

$$A_e = LW + 6H(L + W) + 9\pi H^2 \quad (1)$$

$$N_d = N_g A_e C_1 \times 10^{-6} \quad (2)$$

$$N_c = \frac{1.5\times10^{-3}}{C_2 \times C_3 \times C_4 \times C_5} \quad (3)$$

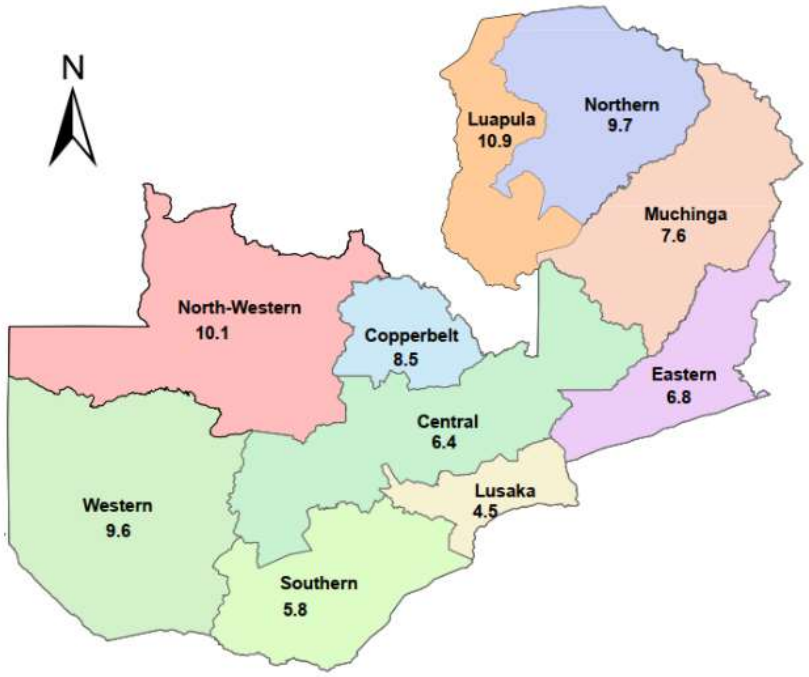

Figure 2. Average lightning flash densities per province in Zambia

With further discussion and analysis, these parameters will go a long way in helping with effective lightning risk assessment and LPS designs in Zambia. The current trend is that the utility companies have been using a keraunic value of 86 thunderstorm days per year to carry out the lightning risk assessment and decide on the LPS design. Thus, the new parameters will provide a new paradigm in LPS designs in the country.

It can be seen in Figure 2 that lightning flash density increases as one moves towards the north of the country. In fact, the national instrumentation surveys have shown that sensitive electronic equipment incur a higher rate of damage as one approaches the northern region, especially that these instruments were not installed with the best practices regarding LPSs. But with the exposure to what ACLENet, SALNet, and lightning protection pioneers are doing, it is possible for Zambia to gain more insight into the protection of infrastructure against the phenomenon. Lightning safety in solar PV installations, power generation, transmission and distribution systems, public transportation and buildings is being promoted through workshops and seminars that attract participation of practitioners from industries and the mines. However, there is still a lot of work to be done especially for rural infrastructure where LPSs are non-existent and communities are left vulnerable to the phenomenon's outbursts. There is a need to ramp up efforts in both urban and peri-urban areas too where it can easily be observed that there are no LPSs installed on a good number of buildings.

*W*uxi University, China

A 3D Corona Discharge Model was developed by Guo et al. (2022). The authors developed a three-dimensional (3D) numerical model for the diffusion of positive corona charges based on a 2D model with a uniform grid to explore the characteristics of corona discharge at a building tip during a thunderstorm in the presence of wind. The variable-grid meshing method is used to solve the problems of implementing a large simulation domain for thunder clouds (kilometer-scale) and the minute calculations of corona discharge at the tip (centimeter scale) in the 3D numerical simulation. The proposed model has advantages in terms of the acquisition of the parameters of corona charges and the spatial distribution of the electric field (E-field) in the environment. We used positive corona discharge at the tip of a building under a negative thunderstorm, along with three wind fields (horizontal wind, updraft, and downdraft with wind speeds of 10 m/s) as an example. The presence of the wind increased the density of corona charges at the tip, where the horizontal wind was the most beneficial for its occurrence. Moreover, the characteristics of distortion of the electric field around the tip were significantly different, owing to the different directions of the wind (Shown as Figure 1). Downdraft led to the maximum enhancement in the E-field above the tip, and updraft prompted the minimum increase in it, by only 1.19 times. However, the opposite results were obtained for the enhancement in the spatial range of the charges: The updraft led to the greatest increase in it, and the downdraft caused the smallest. Corona charges had an apparent shielding effect on the E-field below the tip and can even change the polarity of the E-field in a small area close to it. The strongest shielding effect on the ground E-field occurred in the case of the downdraft, which decreased the E-field to 0.36 times compared with that without the corona charges. On the contrary, corona discharge had the weakest shielding ability on the ground when it met the updraft. The horizontal wind had the largest range of shielding on the ground, of up to 14,699 m^2, while the updraft had the lowest, at only 6,170 m^2.

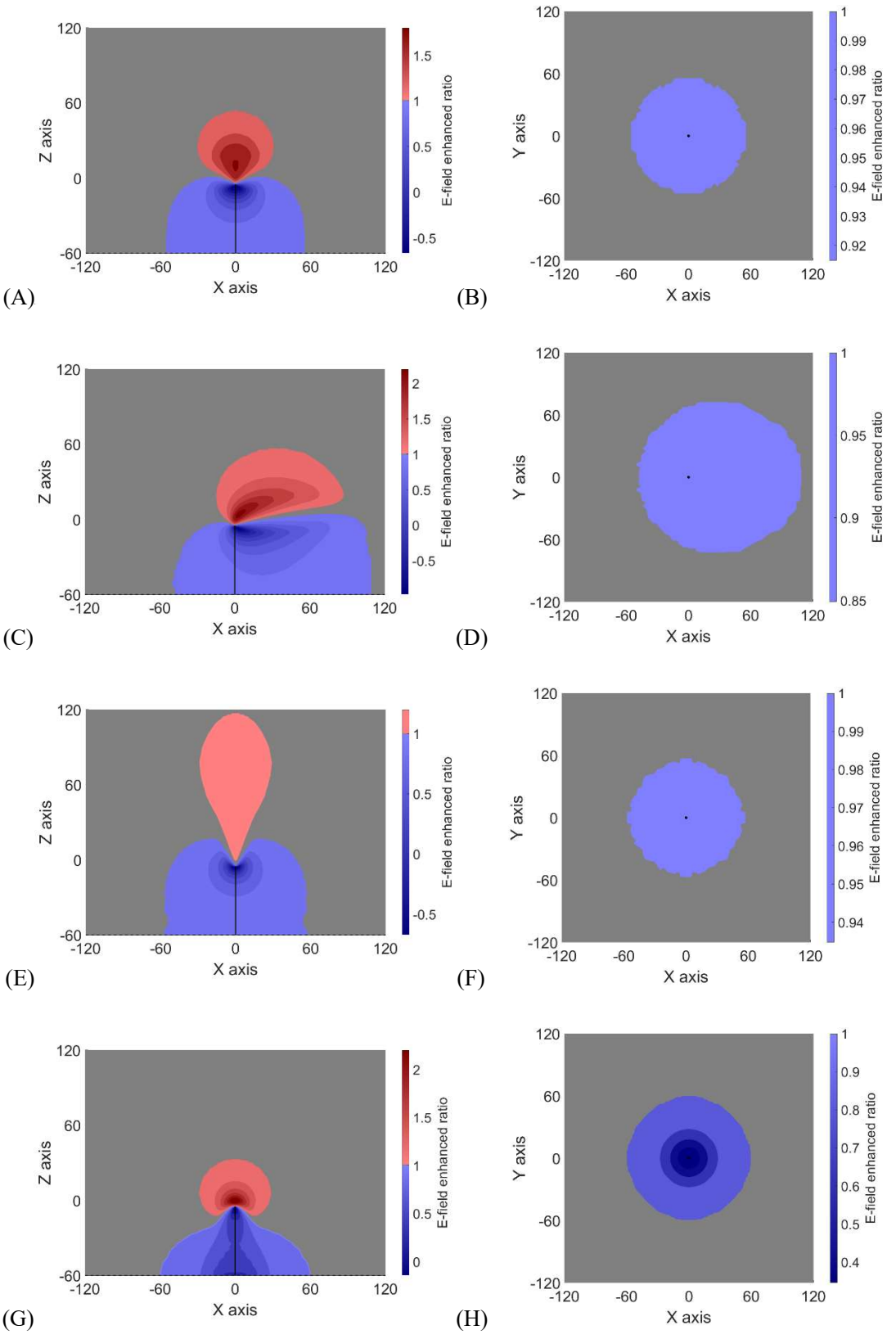

Figure 1. Contours of distortion ($N = \frac{E_{corona}}{E_{original}}$) caused by corona charges in the E-fieldaround the building tip when the thunderstorm background E-field reached its maximum value (20 kV/m). No

wind (A, B). Horizontal wind (C, D). Updraft (E, F). Downdraft (G, H). The left side shows the side views and the right side the top view. E_{corona} is the environmental E-field obtained by considering the corona, and $E_{original}$ is the environmental E-field without the corona. If $N > 1$, this means that the E-field was enhanced by corona discharges; if $0 < N < 1$, it means that the E-field was shielded, and if $N < 0$, it means that the corona ions were too strong such that they prompted a negative enhancement in the E-field.

This list of references is not exhaustive. It includes only papers published during the last six months provided by the authors or found from on-line research in journal websites. Some references of papers very soon published have been provided by their authors and included in the list. The papers in review process, the papers from Proceedings of Conference are not included.

Avila, E., Martinez, L., Pereyra, R., Lang, T., Deierling, W., et al. 2022. Measurements of size and electrical charges carried by precipitation particles during RELAMPAGO field campaign. Earth Space Sci., 9, e2022EA002407. doi:10.1029/2022EA002407.

Behnke, S. A., Edens, H. E., Theiler, J., Swanson, D. J., Senay, S., et al. 2022. Discriminating types of volcanic electrical activity: Toward an eruption detection algorithm. Geophys. Res. Lett., 49, e2022GL099370. doi:10.1029/2022GL099370.

Briggs, M.S., Lesage, S. Schultz, C., Mailyan, B., Holzworth, R.H. 2022. A terrestrial gamma-ray flash from the 2022 Hunga Tonga-Hunga Ha'apai volcanic eruption. Geophys. Res. Lett., 49, e2022GL099660. doi:10.1029/2022GL099660.

Brodehl, S., Mueller, R., Schoemer, E., Spichtinger, P., Wand, M. 2022. End-to-end prediction of lightning events from geostationary satellite images. Remote Sens., 14, 3760. doi:10.3390/rs14153760.

Cheng, S., Wang, J., Cai, L., Zhou, M., Su, R., Huang, Y., Li, Q. 2022. Characterising the dynamic movement of thunderstorms using very low- and low-frequency (VLF/LF) total lightning data over the Pearl River Delta region. Atmos. Chem. Phys., 22, 10045-10059.

Chmielewski, V.C., Blair, J., Kennedy, D., MacGorman, D., Calhoun, K.M. 2022. A comparison of processing methods for the Oklahoma Lightning Mapping Array. Earth Space Sci., 9, e2021EA002081. doi:10.1029/2021EA002081.

Chuang, C.-W., Chen, A.B.-C. 2022. Global distribution and spectral features of intense lightning by the ISUAL experiment. J. Geophys. Res. Atmos., 127, e2022JD036473. doi:10.1029/2022JD036473.

Cooray, V., Cooray, G., Rubinstein, M., Rachidi, F. 2021. Could macroscopic dark matter (Macros) give rise to mini-lightning flashes out of a blue sky without clouds? Atmosphere, 12, 1230. doi:10.3390/atmos12091230.

Cooray, V., Cooray, G., Rubinstein, M., Rachidi, F. 2021. Ionization waves enhance the production of X-rays during streamer collisions. Atmosphere, 12, 1101. doi:10.3390/atmos12091101.

Cooray, V., Cooray, G., Rubinstein, M., Rachidi, F. 2021. On the apparent non-uniqueness of the electromagnetic field components of

return strokes revisited. Atmosphere, 12, 1319. doi:10.3390/atmos12101319.

Cooray, V., Cooray, G., Rubinstein, M., Rachidi, F. 2021. Polarity asymmetry in lightning return stroke speed caused by the momentum associated with radiation. Atmosphere, 12, 1642. doi:10.3390/atmos12121642.

Cooray, V., Jayasinghe, H., Rubinstein, M., Rachidi, F. 2022. The geometry and charge of the streamer bursts generated by lightning rods under the influence of high electric fields. Atmosphere, 13, 2028. doi:10.3390/atmos13122028.

Cooray, V., Rubinstein, M., Rachidi, F. 2022. A self-consistent return stroke model that includes the effect of the ground conductivity at the strike point. Atmosphere, 13, 593. doi:10.3390/atmos13040593.

Cruz, I.T., Saba, M.M.F., Schumann, C., Warner, T.A. 2022. Upward bipolar lightning flashes originated from the connection of recoil leaders with intracloud lightning. Geophys. Res. Lett., 49, 12-19.

Ding, Z., Chen, S., Rakov, V.A., Zhu, Y., Kereszy, I., Uman, M.A. 2022. Comparison of far electric field waveforms produced by rocket-triggered lightning strokes and subsequent strokes in natural lightning. Electric Power Systems Research, Special Issue "Recent Advancements in Lightning Physics, Protection, and Safety", 213, 108784. doi:10.1016/j.epsr.2022.108784.

Du, Y., Zheng, D., Ma, R., Zhang, Y., Lyu, W., et al. 2022. Thunderstorm activity over the Qinghai-Tibet Plateau indicated by the combined data of the FY-2E Geostationary Satellite and WWLLN. Remote Sens., 14, 2855. doi:10.3390/rs14122855.

Dube, A., Maurya, A.K., Dharmaraj, T., Singh, R. 2022. First study of cloud to ground lightning discharges using ground-based observations over Indian subcontinent and its possible relationship with carbon dioxide and aerosols. J. Atmos. Sol.-Terr. Phy., 233, 105890. doi:10.1016/j.jastp.2022.105890.

Fan, Y., Zhang, Y., Lu, G., Lyu, W., Liu, H., Xu, L., Zheng, D. 2022. First measurements of low-medium frequency magnetic radiation for an altitude-triggered lightning flash. Geophys. Res. Lett., 49, e2022GL098867. doi:10.1029/2022GL098867.

Federico, S., Torcasio, R.C., Lagasio, M., Lynn, B.H., Puca, S., Dietrich, S. 2022. A year-long total lightning forecast over Italy with a dynamic lightning scheme and WRF. Remote Sens., 14, 3244. doi:10.3390/rs14143244.

Guo, X., Ji, Z., Gao, Y., Ding, J., Zhang, L. 2022. 3D corona discharge model and its use in the presence of wind during a thunderstorm. Front. Environ. Sci., 10:946020. doi: 10.3389/fenvs.2022.946020.

Gutierrez, G., Castejon, R.M., Tavares, H., Galindo, H., Gil, E.P., et al. 2022. Validation of lightning simulation compared with measurements using DCI technique post-processed to be applied to a lightning threat.

IEEE T. Electromagn C. doi:10.1109/TEMC.2022.3217393.

Handel, S.C., Cummins, K.L., Krider, E.P. 2022. Surface potential gradients and NEXRAD radar reflectivities before the onset of lightning at the KSC-ER. J. Geophys. Res. Atmos., 127, e2022JD036681. doi:10.1029/2022JD036681.

Hayward, L., Whitworth, M., Pepin, N., Dorling, S. 2022. A regional lightning climatology of the UK and Ireland and sensitivity to alternative detection networks. Int. J. Climatol. doi:10.1002/joc.7680.

Heuscher, L., Liu, C., Gatlin, P., Petersen, W.A. 2022. Relationship between lightning, precipitation, and environmental characteristics at mid-/high latitudes from a GLM and GPM perspective. J. Geophys. Res. Atmos., 127, e2022JD036894. doi:10.1029/2022JD036894.

Holle, R.L., Cramer, J.A., Laing, A., Thompson, E.G. Jamaica lightning occurrence, damage, and casualties. 36th International Conference on Lightning Protection (ICLP), 2022, pp. 1-5, doi:10.1109/ICLP56858.2022.9942532.

Huang, H., Wang, D., Yang, J., Wu, T., Takagi, N. 2022. Complicated aspects of a CG lightning flash observed in winter storm in Japan. Journal of Atmospheric Electricity, 41(1), 11-29.

Iudin, D.I., Syssoev, A.A., Rakov, V.A. 2022. Lightning initiation as a consequence of natural thundercloud evolution. Part 1: Role of detachment in the lowering of the air breakdown threshold. Electricity, 11, 13–28.

Iudin, D.I., Syssoev, A.A., Rakov., V.A. 2022. Problems of lightning initiation and development. Radiophysics and Quantum Electronics, 64(11), 780-803.

Kahraman, A., Kendon, E.J., Fowler, H.J., Wilkinson, J.M. 2022. Contrasting future lightning stories across Europe. Environ. Res. Lett., 17, 114023. doi:10.1088/1748-9326/ac9b78.

Kereszy, I., Rakov, V., Czumbil, L., Muresan, A., Ding, Z., et al. 2022. Energetic radiation from subsequent-stroke leaders: The role of reduced air density in decayed lightning channels. Appl. Sci., 12, 7520. doi:10.3390/app12157520.

Kereszy, I., Rakov, V.A., Czumbil, L., Muresan, A., Ding, Z., et al. 2022. Energetic radiation from subsequent-stroke leaders: The role of reduced air density in decayed lightning channels. Appl. Sci., Special Issue "Physics Principles, Measurements and Characteristics of Lightning", 12, 7520. doi:10.3390/app12157520.

Kereszy, I., Rakov, V.A., Ding, Z., Dwyer, J.R. 2022. Ground-based observation of a TGF occurring between opposite polarity strokes of a bipolar cloud-to-ground lightning flash. J. Geophys. Res. Atmos., 127, e2021JD036130. doi:10.1029/2021JD036130.

Kigotsi, J.K., Soula, S., Kazadi, A.B.M., Zana, A.N. 2022. Contribution to the study of

thunderstorms in the Congo Basin: Analysis of periods with intense activity. Atmos. Res., 269, 106013. doi:10.1016/j.atmosres.2021.106013.

Kong, R., Xue, M., Liu, C., Fierro, A.O., Mansell, E.R. 2022. Development of new observation operators for assimilating GOES-R Geostationary Lightning Mapper flash extent density data using GSI EnKF: Tests with two convective events over the United States. Mon. Wea. Rev., 150, 2091-2110.

Kostinskiy, A.Y., Bogatov, N.A., Syssoev, V.S., Mareev, E.A., Andreev, M.G., et al. 2022. Unusual plasma formations produced by positive streamers entering the cloud of negatively charged water droplets. J. Geophys. Res. Atmos., 127, e2021JD035821. doi:10.1029/2021JD035821.

Kutsuna, K., Nagaoka, N., Baba, Y., Tsuboi, T., Rakov, V.A. 2023. Estimation of lightning channel-base current from far electromagnetic field in the case of inclined channel. Electric Power Systems Research, 214, 108854. doi:10.1016/j.epsr.2022.108854.

Lakhdar, A., Mimouni, A., Azzouz, Z.-E. 2022. New approach to revise the spatiotemporal lightning current distribution models intended for tall objects. IEEE T. Electromagn C., 64, 1190-1197.

Lang, T.J., Bang, S.D. 2022. Exploring the scientific utility of combined spaceborne lidar and lightning observations of thunderstorms. Earth Space Sci., 9, e2022EA002400. doi:10.1029/2022EA002400.

Li, Q., Gong, Z., Wang, J., Cai, L., Zhou, M., Fan, Y. 2022. Electric fields calculation of lightning return-strokes in the presence of an attachment point above the ground. J. Atmos. Sol.-Terr. Phy., 237, 105919. doi:10.1016/j.jastp.2022.105919.

Li, Q., Guo, F., Ju, X., Liu, Z., Gan, M., Zhang, K., Cai, B. 2022. Estimation of lightning-generated NOx in the mainland of China based on cloud-to-ground lightning location data. Adv. Atmos. Sci., 40, 129-143.

Li, Y., Zhang, Y., Zhang, Y., Krehbiel, P.R. 2022. Analysis of the configuration relationship between the morphological characteristics of lightning channels and the charge structure based on the localization of VHF radiation sources. Geophys. Res. Lett., 49, e2022GL099586. doi:10.1029/2022GL099586.

Li, Z., Zhang, T., Bao, M., Yu, H., Su, T., Lin, H. 2022. Relationships between cloud-to-ground flashes and ice-phase hydrometeors in a hailstorm. J. Atmos. Sol.-Terr. Phy., 241, 105978. doi:10.1016/j.jastp.2022.105978.

Liu, N., Liu, C., Tissot, Philippe E. 2022. Relative importance of large-scale environmental variables to the world-wide variability of thunderstorms. J. Geophys. Res. Atmos., 127, e2021JD036065. doi:10.1029/2021JD036065.

Liu, X., Zheng, D., Zhang, Y., Zhang, Y., Fan, X., et al. 2022. Spatiotemporal correlation

between artificially triggered and adjacent natural lightning flashes. Remote Sens., 14, 4214. doi:10.3390/rs14174214.

Lu, J., Qie, X., Xiao, X., Jiang, R., Mansell, E.R., Fierro, A.O., et al. 2022. Effects of convective mergers on the evolution of microphysical and electrical activity in a severe squall line simulated by WRF coupled with explicit electrification scheme. J. Geophys. Res. Atmos., 127, e2021JD036398. doi:10.1029/2021JD036398.

Malec, B., Prtenjak, M.T., Horvath, K., Jelic, D., Mikus Jurkovic, P., et al. 2022. Performance of HAILCAST and the lightning potential index in simulating hailstorms in Croatia in a mesoscale model-sensitivity to the PBL and microphysics parameterization schemes. Atmos. Res., 272, 106143. doi:10.1016/j.atmosres.2022.106143.

Manzato, A., Serafin, S., Miglietta, M.M., Kirshbaum, D., Schulz, W. 2022. A Pan-Alpine climatology of lightning and convective initiation. Mon. Wea. Rev., 150, 2213-2230.

Mashao, D.C., Kosch, M.J., Fullekrug, M., Mlynarczyk, J. 2022. Lightning parameters of sprites and diameter of halos over South Africa. J. Atmos. Sol.-Terr. Phy., 240, 105957. doi:10.1016/j.jastp.2022.105957.

Medina, B.L., Carey, L.D., Bitzer, P.M., Lang, T.J., Deierling, W. 2022. The relation of environmental conditions with charge structure in central Argentina thunderstorms. Earth Space Sci., 9, e2021EA002193. doi:10.1029/2021EA002193.

Mohammad, S.A., Ahmad, M.R., Abdullah, M., Sangjong, P., Shamsul Baharin, S.A., et al. 2022. Characteristics of lightning electromagnetic fields produced by Antarctica storms. Atmosphere, 13, 588. doi:10.3390/atmos13040588.

Montanya, J., Lopez, J.A., Van der velde, O., Sola, G., Romero, D., et al. 2022. Potential use of space-based lightning detection in electric power systems. Electric Power Systems Research, 213, 108730.

Oda, P.S.S., Enore, D.P., Mattos, Enrique, V., Goncalves, W.A., Albrecht, Rachel, I. 2022. An initial assessment of the distribution of total Flash Rate Density (FRD) in Brazil from GOES-16 Geostationary Lightning Mapper (GLM) observations. Atmos. Res., 270, 06081. doi:10.1016/j.atmosres.2022.106081.

Osei-Poku, L., Tang, L., Chen, W., Chen, M., Acheampong, A.A. 2022. Comparative study of predominantly daytime and nighttime lightning occurrences and their impact on ionospheric disturbances. Remote Sens., 14, 3209. doi:10.3390/rs14133209.

Peterson, M. 2022. Combined Optical and Radio-Frequency Perspectives on the Time Evolution of Lightning Measured by the FORTE Satellite. Earth Space Sci., 9, e2022EA002281. doi:10.1029/2022EA002281.

Peterson, M. 2022. FORTE measurements of

global lightning altitudes. Earth Space Sci., 9, e2022EA002404. doi:10.1029/2022EA002404.

Peterson, M. 2022. FORTE measurements of global optical lightning waveforms for implications for optical lightning detection. Earth Space Sci., 9, e2022EA002280. doi:10.1029/2022EA002280.

Pizzuti, A., Bennett, A., Soula, S., Amor, S.N., Mlynarczyk, J., Fuellekrug, M., Pedeboy, S. 2022. On the relationship between lightning superbolts and TLEs in Northern Europe. Atmos. Res., 270, 106047. doi:10.1016/j.atmosres.2022.106047.

Poreba, S., Taszarek, M., Ustrnul, Z. 2022. Diurnal and seasonal variability of ERA5 convective parameters in relation to lightning flash rates in Poland. Weather Forecast., 37, 1447-1470.

Pracser, E., Bozoki, T. 2022. On the reliability of the inversion aimed to reconstruct global lightning activity based on Schumann resonance measurements. J. Atmos. Sol.-Terr. Phy., 235, 105892. doi:10.1016/j.jastp.2022.105892.

Qie, X., Qie, K., Wei, L., Zhu, K., Sun, Z., et al. 2022. Significantly increased lightning activity over the Tibetan Plateau and its relation to thunderstorm genesis. Geophys. Res. Lett., 49, e2022GL099894. doi:10.1029/2022GL099894.

Qie, X., Wei, L., Zhu, K., Qie, K., Xu, C., et al. 2022. Regional differences of convection structure of thunderclouds over the Tibetan Plateau. Atmos. Res., 278, 106338. doi:10.1016/j.atmosres.2022.106338.

Rakov, V.A., Kereszy, I. 2022. Ground-based observations of lightning-related X-ray/gamma-ray emissions in Florida: Occurrence context and new insights. Electr. Pow. Syst. Res., 213, 108736. doi:10.1016/j.epsr.2022.108736.

Rakov, V.A., Tran, M.D., Zhu, Y., Ding, Z., Leal, A.F.R., et al. 2022. New insights into the lightning discharge processes. Plasma Sources Science and Technology (PSST), Special Issue in Memory of Yuri Raizer, 31, 104005, 17p. doi:10.1088/1361-6595/ac9330.

Sabri, M.H.M., Ahmad, M.R., Al-Kahtani, A.A.N., Ab Kadir, M.Z.A., Baharin, S.A.S., et al. 2022. A study of cloud-to-ground lightning flashes initiated by fast positive breakdown. Atmos. Res., 276, 106260. doi:10.1016/j.atmosres.2022.106260.

Sabri, M.H.M., Alkahtani, A.A., Ahmad, M.R., Baharin, S.A.S., Lu, G., et al. 2022. Microwave radiation associated with lightning initiation events of negative cloud-to-ground flashes. Atmosphere, 13, 1454. doi:10.3390/atmos13091454.

Sharma, S., Neupane, B., KC, H.B., Koirala, M.P., Damase, N.P., et al. 2022. Lightning threats in Nepal: Occurrence and human impacts. Geomatics, Natural Hazards and Risk, 13, 1-18.

Shi, Z., Hu, J., Tan, Y., Guo, X., Wang, H., et al.

2022. Significant influence of aerosol on cloud-to-ground lightning in the Sichuan Basin. Atmos. Res., 278, 106330. doi:10.1016/j.atmosres.2022.106330.

Skeie, C.A., Ostgaard, N., Mezentsev, A., Bjorge-Engeland, I., Marisaldi, M., et al. 2022. The temporal relationship between terrestrial gamma-ray flashes and associated optical pulses from lightning. J. Geophys. Res. Atmos., 127, e2022JD037128. doi:10.1029/2022JD037128.

Solimine, S.L., Zhou, L., Raghavendra, A., Cai, Y. 2022. Relationships between intense convection, lightning, and rainfall over the interior Congo Basin using TRMM data. Atmos. Res., 273, 106164. doi:10.1016/j.atmosres.2022.106164.

Springsklee, C., Scheu, B., Manga, M., Cigala, V, Cimarelli, C., Dingwell, D.B. 2022. The influence of grain size distribution on laboratory-generated Volcanic lightning. J. Geophys. Res. Solid Earth, 127, e2022JB024390. doi:10.1029/2022JB024390.

Stephan, K.D., Sonnenfeld, R., Keul, A.G. 2022. First comparisons of ball-lightning report website data with lightning-location-network data. J. Atmos. Sol.-Terr. Phy., 240, 105953. doi:10.1016/j.jastp.2022.105953.

Tian, Y., Yao, W., Sun, Y., Wang, Y., Liu, X., et al. 2022. A method for improving the performance of the 2a lightning jump algorithm for nowcasting hail. Atmos. Res., 280, 106404. doi:10.1016/j.atmosres.2022.106404.

Tiberia, A., Arnone, E., Ursi, A., Fuschino, F., Virgilli, E., et al. 2022. A joint LINET and ISS-LIS view of lightning distribution over the Mt. Cimone area within the GAMMA-FLASH program. Remote Sens., 14, 3501. doi:10.3390/rs14143501.

Tinsley, B.A. 2022. Uncertainties in evaluating global electric circuit interactions with atmospheric clouds and aerosols, and consequences for radiation and dynamics. J. Geophys. Res. Atmos., 127, e2021JD035954. doi:10.1029/2021JD035954.

Urbani, M., Montanya, J., van der Velde, O.A., Arcanjo, M., Lopez, J.A. 2022. Multi-stroke positive cloud-to-ground lightning sharing the same channel observed with a VHF broadband interferometer. Geophys. Res. Lett., 49, e2021GL097272. doi:10.1029/2021GL097272.

Utsav, B., Deshpande, S.M., Das, S.K., Pawar, S.D., Pandithurai, G. 2022. Relationship between convective storm properties and lightning over the Western Ghats. Earth Space Sci., 9, e2022EA002232. doi:10.1029/2022EA002232.

Vani, G.K., Mohan, G.M., Hazra, A., Pawar, S.D., Pokhrel, S. et al. 2022. Evaluation and usefulness of lightning forecasts made with lightning parameterization schemes coupled with the WRF model. Weather Forecast., 37, 709-726.

Wang, D., Wu, T., Huang, H., Yang, J.,

Yamamoto, K. 2022. 3D mapping of winter lightning in Japan with an array of discone antennas. IEEJ T. Electr. Electr., 17, 1606-1612.

Wang, X., Wang, H., Lyu, W., Chen, L., Ma, Y., et al. 2022. First experimental verification of opacity for the lightning near-infrared spectrum. Geophys. Res. Lett., 49, e2022GL098883. doi:10.1029/2022GL098883.

Watanabe, N., Nag, A., Diendorfer, G., Pichler, H., Schulz, W., Rassoul, H.K. 2022. Characterization of the initial stage in upward lightning at the Gaisberg Tower: 2. Electric field signatures. Electr. Pow. Syst. Res., 213, 108627. doi:10.1016/j.epsr.2022.108627.

Wu, T., Wang, D., Takagi, N. 2022. On the intensity of first return strokes in positive cloud-to-ground lightning in winter. J. Geophys. Res. Atmos., 127, e2022JD037282. doi:10.1029/2022JD037282.

Xu, L., Zhang, W., Cao, X., Zhao, J., Zhang, Y. 2022. A 10-year thundersnow climatology over China. Geophys. Res. Lett., 49, e2022GL100734. doi:10.1029/2022GL100734.

Xu, M., Qie, X., Pang, W., Shi, G., Liang, L. et al. 2022. Lightning climatology across the Chinese continent from 2010 to 2020. Atmos. Res., 275, 106251. doi:10.1016/j.atmosres.2022.106251.

Yair, Y.Y., Lynn, B.H., Korzets, M., Jaffe, M. 2022. The "weekend effect" in lightning activity during winter thunderstorms over the Tel-Aviv, Israel, Metropolitan Area. Atmosphere, 13, 1570. doi:10.3390/atmos13101570.

Zhang, M., Lu, G., Wang, Z., Peng, K.-M., Huang, H., et al. 2022. Sprite distribution of different polarities from ISUAL observations with machine learning method. J. Geophys. Res. Atmos., 127, e2022JD036968. doi:10.1029/2022JD036968.

Zhang, W., Zhang, Y., Shu, S., Zheng, D., Xu, L. 2022. Lightning distribution in tropical cyclones making landfall in China. Front. Earth Sci., 10, 940205. doi:10.3389/feart.2022.940205.

Zheng, T., Tan, Y., Wang, H., Shi, Z., Lyu, W., et al. 2022. A self-sustained charge neutrality intracloud lightning parameterization containing channel decay and reactivation. Geophys. Res. Lett., 49, e2022GL100849. doi:10.1029/2022GL100849.

Zhu, Y., Stock, M., Lapierre, J., DiGangi, E. 2022. Upgrades of the Earth Networks Total Lightning Network in 2021. Remote Sens., 14, 2209. doi:10.3390/rs14092209.

Atmospheric Electricity

https://www.iamas.org/icae/

NEWSLETTER

Vol.33 NO.2 Nov 2022

Edited by: Wenjuan Zhang (CAMS) and Haiyang Gao (NUIST)

REMINDER

Newsletter on Atmospheric Electricity presents twice a year (May and November) to the members of our community with the following information:

- ✧ announcements concerning people from atmospheric electricity community, especially awards, new books...,
- ✧ announcements about conferences, meetings, symposia, workshops in our field of interest,
- ✧ brief synthetic reports about the research activities conducted by the various organizations working in atmospheric electricity throughout the world, and presented by the groups where this research is performed, and
- ✧ a list of recent publications. In this last item will be listed the references of the papers published in our field of interest during the past six months by the research groups, or to be published very soon, that wish to release this information, but we do not include the contributions in the proceedings of the Conferences.

No publication of scientific paper is done in this Newsletter. We urge all the groups interested to submit a short text (one page maximum with photos eventually) on their research, their results or their projects, along with a list of references of their papers published during the past six months. This list will appear in the last item. Any information about meetings, conferences or others which we would not be aware of will be welcome.

Call for contributions to the newsletter

All issues of this newsletter are open for general contributions. If you would like to contribute any science highlight or workshop report, please contact Weitao Lyu (wtlu@ustc.edu) preferably by e-mail as an attached word document.

The deadline for **2023 spring issue** of the newsletter is **May 15, 2023**.

PRESIDENT

Xiushu Qie

Chinese Academy of Sciences

E-mail: qiex@mail.iap.ac.cn

SECRETARY

Weitao Lyu

Chinese Academy of Meteorological Sciences

E-mail: wtlu@ustc.edu